Chapter 2

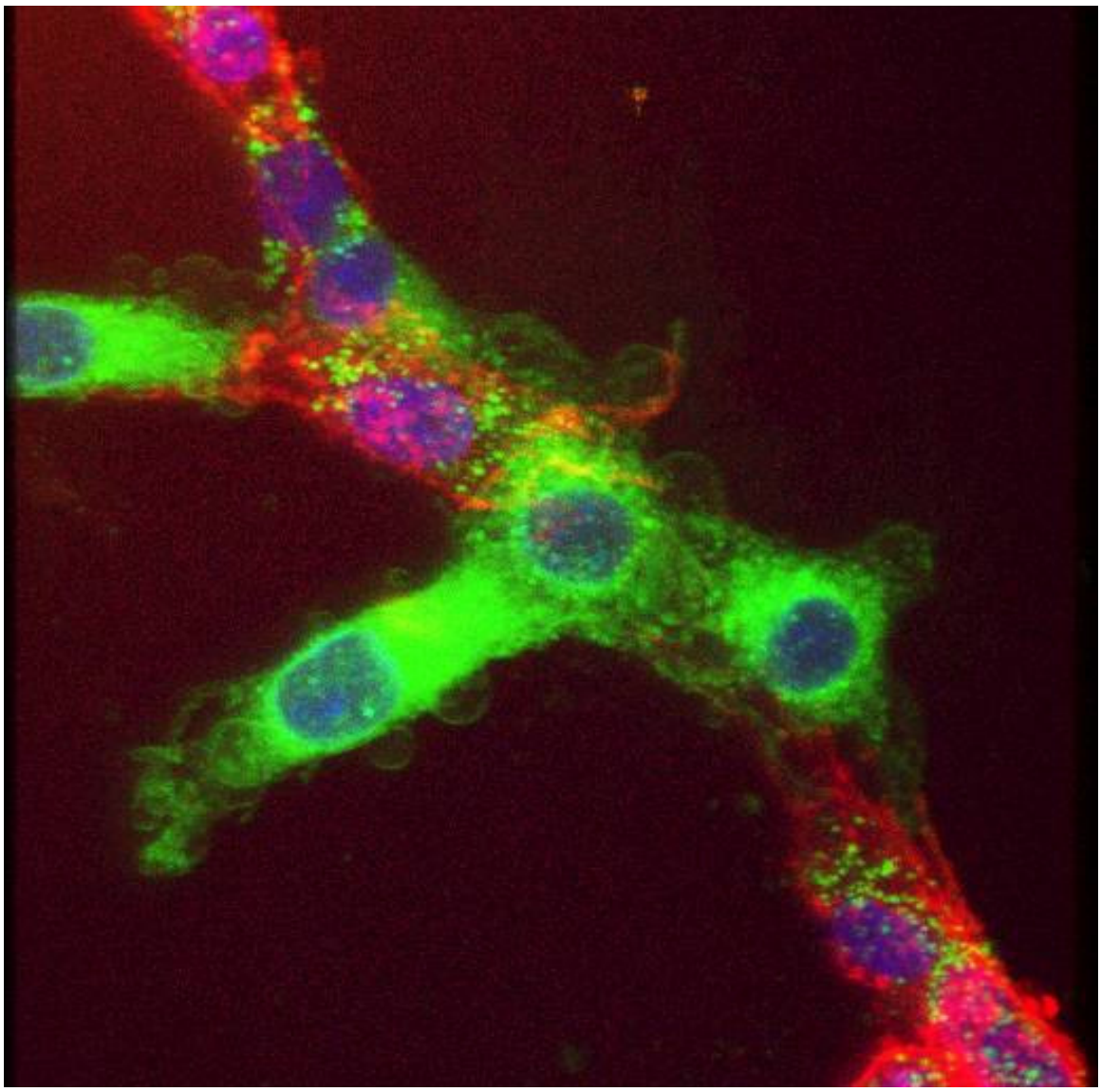

Evaluation of cell adhesion and growth on pSi surfaces

Chapter outline

pSi has been used previously for *in vitro* cell culture studies where the influence of chemical and topographical properties and the biodegradability of the material were investigated[1-12]. PC12 and rat primary hepatocytes growing on pSi surface generally showed good viability over extended period of time and cell morphology and behaviour were found to be influenced by the surface topography and chemistry. Furthermore, the surfaces do not show any cytotoxic effects to the cell culture upon surface degradation. Other attractive features of pSi include the large surface area of hundreds of m^2 per gram material and tunable degradation rate from hours to months. These attributes have contributed to the selection of pSi as a degradable biomaterial for tissue engineering[13-15].

In this chapter, we will investigate:

2.1 Mammalian cell adhesion and growth on surface modified pSi films in short term culture

2.2 Long term culture and functional characterisation of primary hepatocyte cells on pSi films

2.1 Mammalian cell adhesion and growth on surface modified pSi films in short term culture

Biomaterials for tissue engineering applications in vivo have to sustain the attachment, growth and function of primary cells for extended periods of time[16-18]. In order to design appropriate materials, one has to appreciate that different cells respond differently to biological/chemical[19-21] and physical cues[22, 23], even when under similar culture conditions. There is no biomaterial that fits all cells. Instead biomaterial properties have to be fine-tuned for a particular cell type. The identification and characterization of these surface parameters is therefore an important aspect of biomaterials research. Materials with low toxicity yet tuneable surface chemistry and topography are very useful for such investigations.

In recent years, pSi has gained increasing recognition as a biomaterial candidate that enables chemical and physical modifications to be easily performed upon. Reports on using pSi in biomaterial applications have been very encouraging[3, 5, 9]. pSi can be easily fabricated with the desired nanostructured architectures by modulating the anodisation conditions. Pore size, porosity and film thickness is determined by the anodisation conditions during fabrication. Furthermore, the surface chemistry of pSi can be altered by simple methods such as thermal oxidation, ozonolysis and straightforward reactions such as silanisation and hydrosilylation[8, 24, 25]. The physical characteristics (pore size and porosity) and the surface chemistry then control the degradation behaviour of pSi in aqueous medium.

It is well known that adhering cells receive both chemical and physical cues from the surfaces with which they are in contact[19, 21, 26, 27]. When using nanostructured materials such as pSi, it is important to discern between surface chemistry and physical surface attributes and consider their influences on cellular traits separately. This distinction between chemical and physical

cues from pSi films will be made in this thesis. In this chapter, we will investigate the effects of surface chemistry on cell behaviour in this section while the effects of physical cues will be addressed in later chapters.

2.1.1 Materials and methods

All commerically available chemical reagents were used without purificiation. 3-Aminopropyltrimethoxysilane (APTMS) were purchased from **Sigma.** Dulbecco's modified Eagles' medium (DMEM), fetal bovine serum (FBS) and penicillin/streptomycin solution were acquired from **Sigma**. N-(triethoxysilylpropyl)-O-polyethylene oxide urethane (PEG) was purchased from **Gelest Inc.** while rat Type I Collagen and XTT toxicology assay kit was obtained from **Sigma.** EtOH (100%) and dichloromethane (DCM) were purchased from **ChemSupply** while acetone and toluene were acquired from **Ajax Fine Chemicals.** HF (49%) was acquired from **Merck**.

2.1.1.1 Etching procedure

Heavily doped p-type silicon wafers (B-doped, orientation (100)) from **Silicon Quest** (Santa Clara, CA, USA) with a resistivity of 3-6 Ω·cm were used to fabricate porous silicon via an anodic etch with a 1:1 EtOH:HF solution (reconstituted from 49% HF solution). The back of the porous silicon wafer was contacted onto aluminium foil (**British Drug Houses (BDH)**) and mounted in a custom-made Teflon etching cell having an O-ring with an opening diameter of 1.5 cm. Anodization was performed in the dark at a current density of 44 mA/cm^2 for 2 minutes. After etching, the porous silicon substrates were washed with methanol, acetone and dichloromethane before being dried under a stream of nitrogen.

2.1.1.2 Surface preparation

To investigate the effects of surface chemistry on the adhering cells, 6 different surface conditions was employed: Freshly etched, ozone oxidized, APTMS functionalised, PEG functionalised, FBS coated and collagen coated. Freshly etched pSi surfaces of hydride terminus were expected to degrade relatively rapidly in aqueous condition while ozone oxidised surfaces have similar chemistry to those of glass. APTMS functionalised surfaces will have amine terminated groups on the surface that can promote cell adhesion while PEG functionalisation has anti-biofouling properties. Both FBS and collagen coated surfaces will be expected to improve cell adhesion on the surface. The freshly etched pSi surfaces were used without further modification while the other surfaces were ozone oxidised using a Fischer OZON Ozon-Generator 500 for 20 minutes at ozone rate of 3.25 g h^{-1}. After oxidation, the surfaces were rinsed extensively with EtOH and dried under a stream of N_2.

For the APTMS samples, the surfaces were functionalised with APTMS silane at 50 mM in 5 mls of distilled toluene for 20 mins at room temperature. The APTMS surfaces were subsequently rinsed with 95% EtOH and dried under N_2. For the PEG surfaces, the surfaces were incubated with 50 mM PEG silane in toluene for 18 hours under argon at 70ºC. The PEG functionalised surfaces were subsequently rinsed with 95% EtOH and dried under N_2. Collagen (10 mg) in 0.1M acetic acid was applied drop-wise on pSi wafers until the surface was completely covered and subsequently allowed to evaporate in the laminar flow hood (**Nuaire 120**). The surfaces sterilised via exposure to ultraviolet light (253.7 nm) overnight in the laminar flow hood. For FBS treatment of pSi, 50 ml of a 10% (vol/vol) solution of FBS in filter sterilised 10 mM 1X PBS (0.014 mM NaCl, 0.27 mM KCl, 0.8 mM Na_2HPO_4 and

0.8 mM KH_2PO_4 and adjusted to pH 7.4) was also deposited drop wise onto 95% EtOH sterilised pieces of oxidised pSi and allowed to dry onto the surface[9].

2.1.1.3 Atomic Force Microscopy (AFM)

Atomic force microscopy (AFM) was performed on all 6 surfaces using a Multimode Nanoscope IV (Veeco Instruments Ltd.) operating in tapping mode in air. Silicon tips (FESP, Digital Instruments) with a resonance frequency of 50–70 kHz were used at a free oscillation amplitude of 2V. Nanoscope III v5.30r3 software was used to perform offline analysis of the images.

2.1.1.4 Diffusion Reflectance Infrared Spectroscopy

Spectra were acquired in diffuse reflectance (DRIFT) mode with a BioRad digital division FTS-40A, fitted with an ESC DRIFT compartment. The sample compartment was purged with nitrogen with flat unmodified silicon being used as the background before recording spectra of the modified surfaces (duplicates) in Kubelka-Munk units at a resolution of 4 cm^{-1}.

2.1.1.5 Surface degradation studies

Degradation studies of 6 different pSi surfaces were performed using interferometric reflectance spectroscopy (Ocean Optics S2000 with illumination by a tungsten halogen light

source) to determine changes to the effective optical thickness of pSi from hydrolytic degradation in 1X PBS at pH 7.4. The optical thickness was calculated using Fourier transformation of the fringe patterns of the reflectance spectrum of the pSi surface. Changes in effective optical thickness were monitored over a period of 60 mins.

2.1.1.6 Cell culture

Prior to cell culture, freshly etched, oxidised, APTMS and PEG functionalised pSi surfaces were extensively washed with EtOH and dried with N_2 in a laminar flow hood. FBS and collagen coated surface were used directly after sterilisation under UV in the laminar flow hood. The pSi surfaces were transferred onto sterile 6-well plates. Next, 2 mL of rat pheochromocytoma cells (PC12) at a density of about 1.46 x 10^6/mL (determined from haemocytometer) was seeded on each of the surface and were incubated in Dulbecco's Eagle Medium (DMEM) supplemented with 10 % FBS and 50 IU/ml penicillin/streptomycin and subsequently adjusted to pH of 7.2 at 37°C for 24 h. At the end of the incubation time, 10 µL of 15 mg/mL of fluorescein diacetate (FDA) in acetone were added to the medium and incubated at room temperature for 10 min. All surfaces were performed in duplicate in 12-well plates. The surfaces were subsequently washed with 1X PBS. Cell attachment was observed using a Leitz fluorescence microscope under an excitation wavelength of 495 nm.

2.1.1.7 Cell viability studies

XTT cytotoxicity tests were carried out on cell culture from the 6 different surfaces and also on a flat silicon wafer (control) to study the viability of the cells over 6, 12 and 24 hours. 1

ml of PC12 cell suspension in DMEM supplemented with 10% FBS at a density of about 1.46 x 10^6/ml was first seeded on each of the surfaces on 6 well plates and was incubated at 37 °C. After 6 hours, 0.2 mls of reconstituted XTT in DMEM were added to each of the wells and the culture plates were returned back to the incubator for another 2 hours. After the incubation, 1 ml of the cell suspension was carefully removed from each well and 100 µl aliquot was dispensed onto a 96-well plate. The absorbance of the solution was measured with a Vmax kinetic microplate reader (**Molecular Devices**) both at a wavelength of 450 nm and 650 nm. This experiment was repeated for both 12 hour and 24 hour culture times. The normalised absorbance value was derived from the subtraction of the absorbance at 450 nm with the background absorbance at 650 nm. All sampling was performed in triplicate.

2.1.2 Results and Discussion

2.1.2.1 Surface characterisation

After modifications on the pSi surfaces, AFM was performed in order to determine how the surface modifications affect the topography of the pSi films. AFM analysis of the freshly etched surface (figure 2.1 (a)) showed that the average pore size obtain from for the applied anodisation conditions was 25 nm. Such mesoporous pSi films are mechanically stable and are suitable for this cell culture investigation. AFM analysis also showed very little change in topographical characteristics between freshly etched, oxidised and PEG silanised surfaces (figure 2.1 (a), (b) and (d)). However, for the APTMS surfaces, we observed the formation of numerous small aggregates dispersed throughout the surface (figure 2.1 (c)). It is important to note that the silanisation time employed for this experiment was much longer (20 mins) than the times reported in literature and this may contribute to the aggregation of the APTMS silane. Coating pSi surface with FBS did not result in any notable protein aggregates on the surface (figure 2.1 (e) unlike those from the collagen surfaces (figure 2.1 (f)). However it was not easy to discern the surface pores from the FBS coated surface. This may be due to the deposition of small proteins in the pores as previously reported in literature[9]. Finally, large and often elongated aggregates (400-700 nm) were seen on collagen coated pSi surfaces (figure 2.1 (f)).

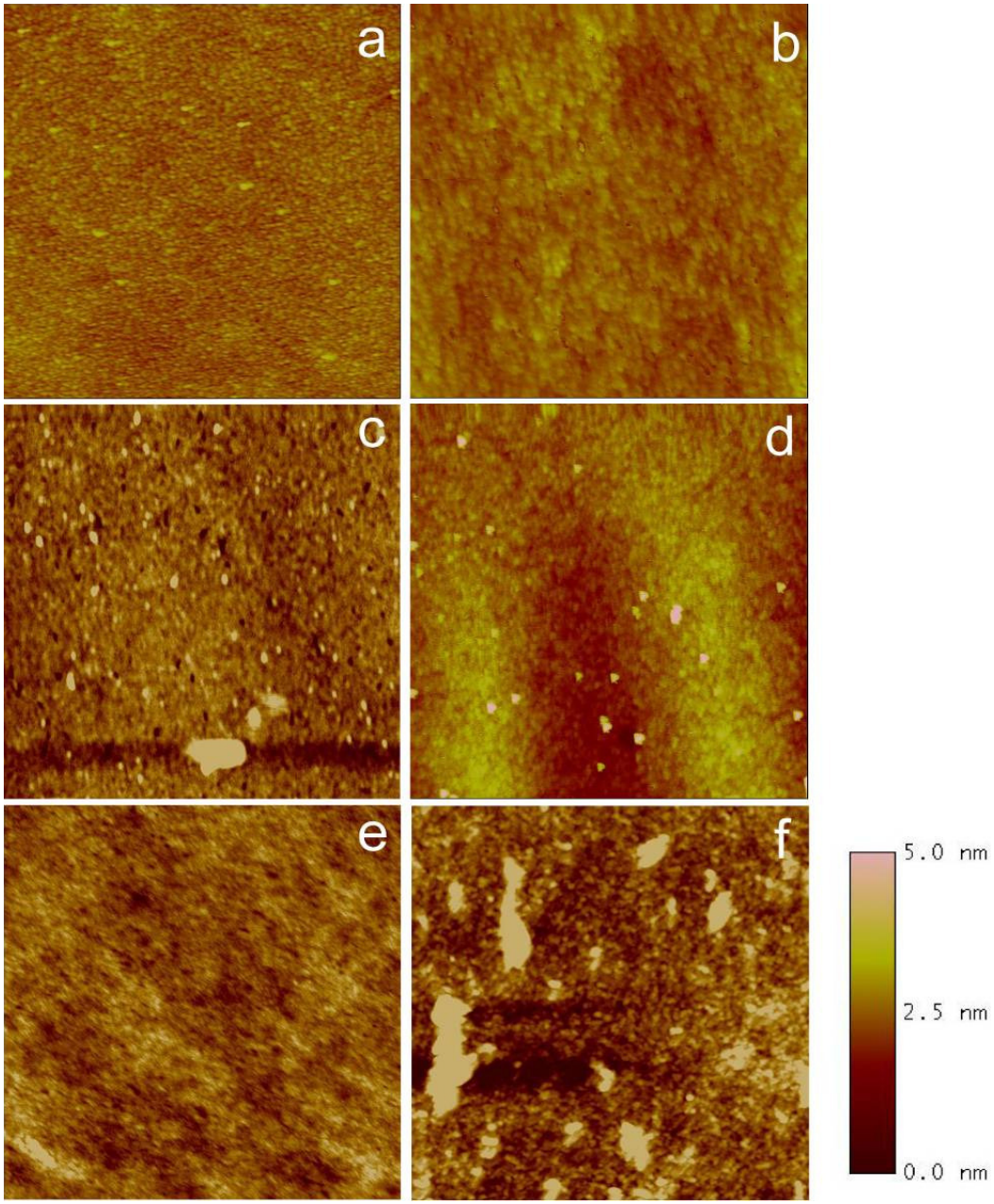

Figure 2.1- AFM analysis of the modified pSi surfaces for (a) Freshly etched, (b) ozone oxidised, (c) APTMS silanised, (d) PEG silanised, (e) FBS coated and (f) collagen coated. All images are 2 µm in size.

The area statistical root mean square roughness (rms roughness) values for all 6 samples were also measured from an image size of 500 nm in duplicate. Both freshly etched and oxidised surfaces showed very similar rms roughness values of 0.16 and 0.20 nm, respectively. The rms roughness value found for the PEG silane was 0.19 nm and suggested the PEG silanisation did not change the roughness on the pSi surface. However the rms roughness

value for APTMS sample was samples were found to be rougher, with rms values of 0.34 nm for APTMS. Coating pSi with FBS resulted in a surface with a rms roughness value of 0.38 nm. The collagen coated surfaces have the highest rms values, at 1.50 nm. From this, we can conclude that while protein deposition such as FBS and collagen modification on the surfaces increase the roughness considerably, ozone oxidization and PEG silanisation did not change the surfaces roughness. We had also noticed a substantial increase of surface roughness from APTMS silanisation, from 0.16 nm (freshly etched) to 0.34 nm (APTMS) and this may be attributed to the fact that the silane may have polymerised and formed aggregates on the surface during the 20 min reaction time, thus contributing to the overall roughness.

The modifications on the surfaces were further confirmed by DRIFT-IR spectroscopy. As shown in figure 2.2 (a), freshly etched pSi surface exhibits bands at ~2100 cm^{-1} and these are the stretching modes of Si-H_x (x = 1,2,3)[8]. These were replaced by a peak at 1083 cm^{-1} and a shoulder at 1170 cm^{-1} attributed to an asymmetrical Si-O-Si and Si-OH stretching modes, respectively upon ozone oxidation (Fig. 2.2 (b))[28-30]. Silanisation with the APTMS silane led to the appearance of multiple peaks centered between 1540-1645 cm^{-1} which corresponds to N-H amide bending vibration (figure 2.2 (c)). Silanisation with PEG led to the appearance of two prominent peaks, one at 1530 cm^{-1} corresponding to the urethane C-N stretching vibrational mode and another at 1705 cm^{-1} that corresponds to the urethane C=O stretching vibration (figure 2.2 (d)). The FBS coated surfaces (figure 2.2 (e)) had a prominent N-H amide band at 1600 cm^{-1}, confirming the presence of proteins absorbed onto the surface. However, this band was very weak on the collagen-coated surface, perhaps indicating a patchy surface coverage which is consistent with the AFM images (figure 2.2 (f)).

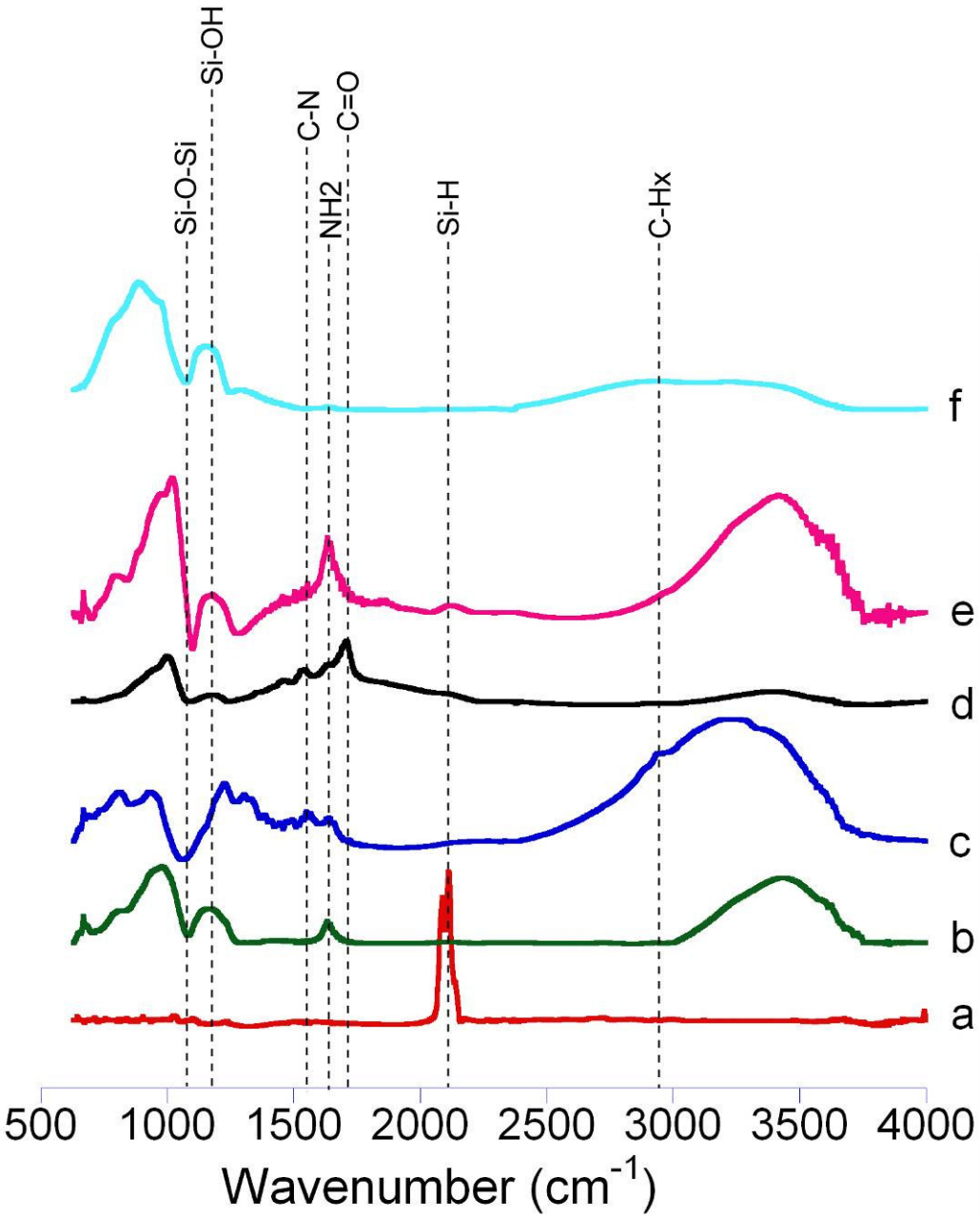

Figure 2.2 - Diffuse reflectance IR (DRIFT-IR) spectra of the 6 surfaces. (a) Freshly etched, (b) ozone oxidised, (c) APTMS silanised, (d) PEG silanised, (e) FBS coated and (f) collagen coated pSi surfaces.

The stability of the films that underwent these modifications was investigated by measuring the rate of hydrolytic degradation of the film in aqueous neutral medium. The change in the effective optical thickness of the film over a course of 60 mins in 1X PBS was measured by means of interferometric reflectance spectroscopy and the data is as shown in figure 2.3. The optical thickness is proportional to the product of film thickness and refractive index. A

decrease in optical thickness in aqueous environment is caused by oxidation of silicon to silica or silicon dissolution (resulting in a refractive index decrease) of the porous medium or pore collapse (resulting in a decrease of film thickness). Freshly etched surface was found be to very highly unstable in PBS and registered a loss of nearly 7% in optical thickness over the course of 60 mins. Ozone oxidization was found to increase the stability of the pSi film significantly, while this stability was further improved by the collagen coating. PEG and APTMS functionalised surfaces were very stable and there were no notable changes in the optical thickness during the time. Interestingly, FBS coating on the oxidised surface was found to also confer stability similar to those that had been functionalised with the alkyl silane, indicating that a dense protective protein layer has formed on the surface, consistent with the IR results.

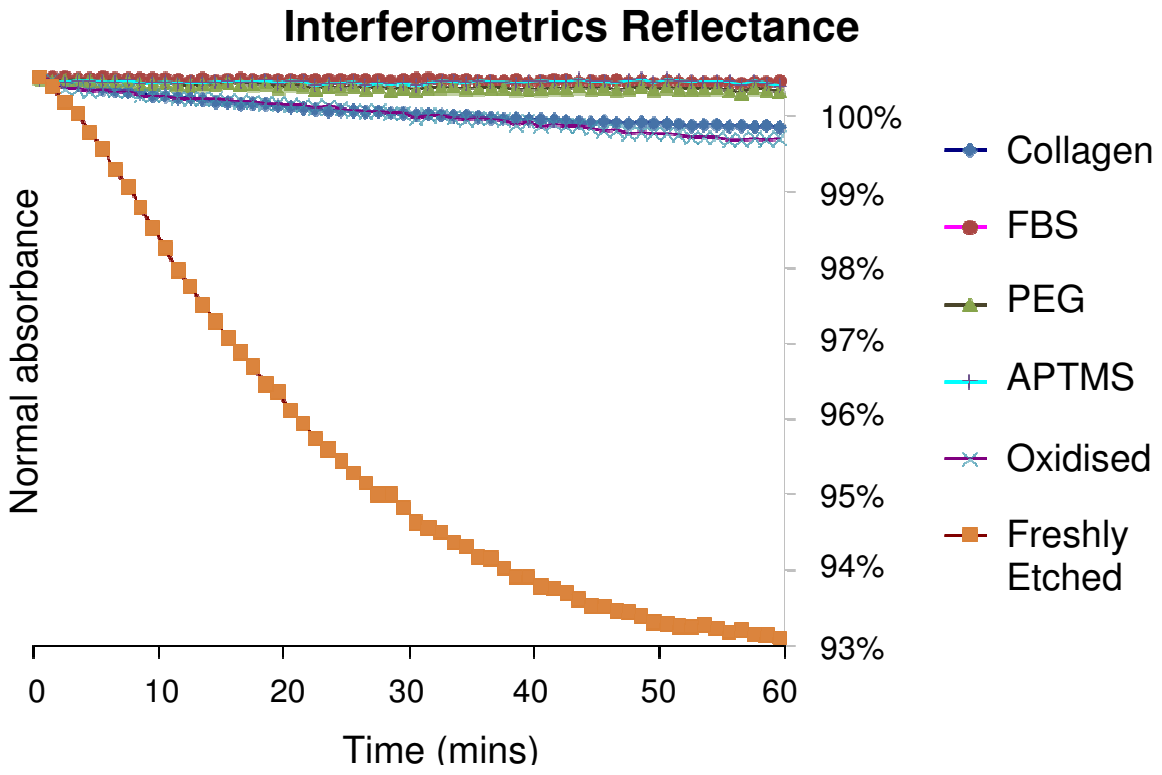

Figure 2.3 – The change in optical thickness of the modified pSi surfaces over 60 mins in 1X PBS.

2.1.2.2 Cell culture

PC12 is a neuronal-like cell line that has an elongated cell morphology when cultured on flat surfaces. Due to its enlongated cell morphology, changes to its cellular morphology can be easily observed[31], thus rendering it is an ideal cell candidate for studying the effects of surface chemistry on cell adhesion. After 24 hours of incubation, the morphology of PC12 cells stained with the viability stain FDA on the 6 different surfaces was examined under the fluorescence microscope. A flat silicon surface was also used as the experimental control. The fluorescence images of the cell morphology are shown in figure 2.4.

After 24 hours of incubation, PC12 cells were observed being oviod well-spread on the flat silicon surfaces and displaying its typical neuronal-like cell morphology with neuronal processes extending out from the cell body (figure 2.4 (a)). There were only a few cells observable under the fluorescence microscope on the freshly etched pSi surfaces. This was most likely to be due to the rapid degradation of pSi in the culture medium which prevented cell attachment. The few cells detected on the surface generally exhibited an ovoid appearance. On oxidised pSi surfaces, there were only a few cells that were observable under the fluorescence microscope. This discouragement of cell adhesion on the surface was presumably due to the hydrophilic nature of the oxidised pSi, preventing protein adsorption, but pSi corrosion during cell culture could also be a contributing factor. The morphology of these cells was generally rounded and cells were observed to form clusters (figure 2.4 (c)). APTMS silanisation encouraged cell attachments as a large number of cells were found attaching on the pSi surface (figure 2.4 (d)). This observation was within expectation as amine functionalised surfaces had been known to promote cell attachment[9, 32]. However, it is important to note that despite the high number of cells detected on these surfaces, the cells

generally displayed a rather ovoid morphology unlike the elongated morphology observed from the flat silicon. PEG functionalisation is generally seen to create a non-biofouling surface that can strongly discourage cell attachment[7]. This was confirmed for PEG functionalised pSi (see figure 2.4 (e)). After 24 hours, there were very few cells observed on the PEG silanised surfaces and these cells were generally round in appearance and often clustered together.

By coating the surface with FBS, fluorescence microscopy revealed that cell attachment was strongly encouraged (figure 2.4 (f)). There were many cells attached on these surfaces but we noticed a different adhesion behavior. There was considerably less clustering of the cells as compared to the flat and the APTMS surfaces. This may suggest that while cell attachment was encouraged on these FBS coated surfaces, the presence of FBS proteins on both surface and solution may have a negating effect on the promotion of neuronal processes, as reported previously in the literature[33]. Lastly, the collagen coated surfaces were found to be highly favorable towards cell attachment and the morphology of the cells on these surfaces closely resembled that of cells cultured on the flat surface.

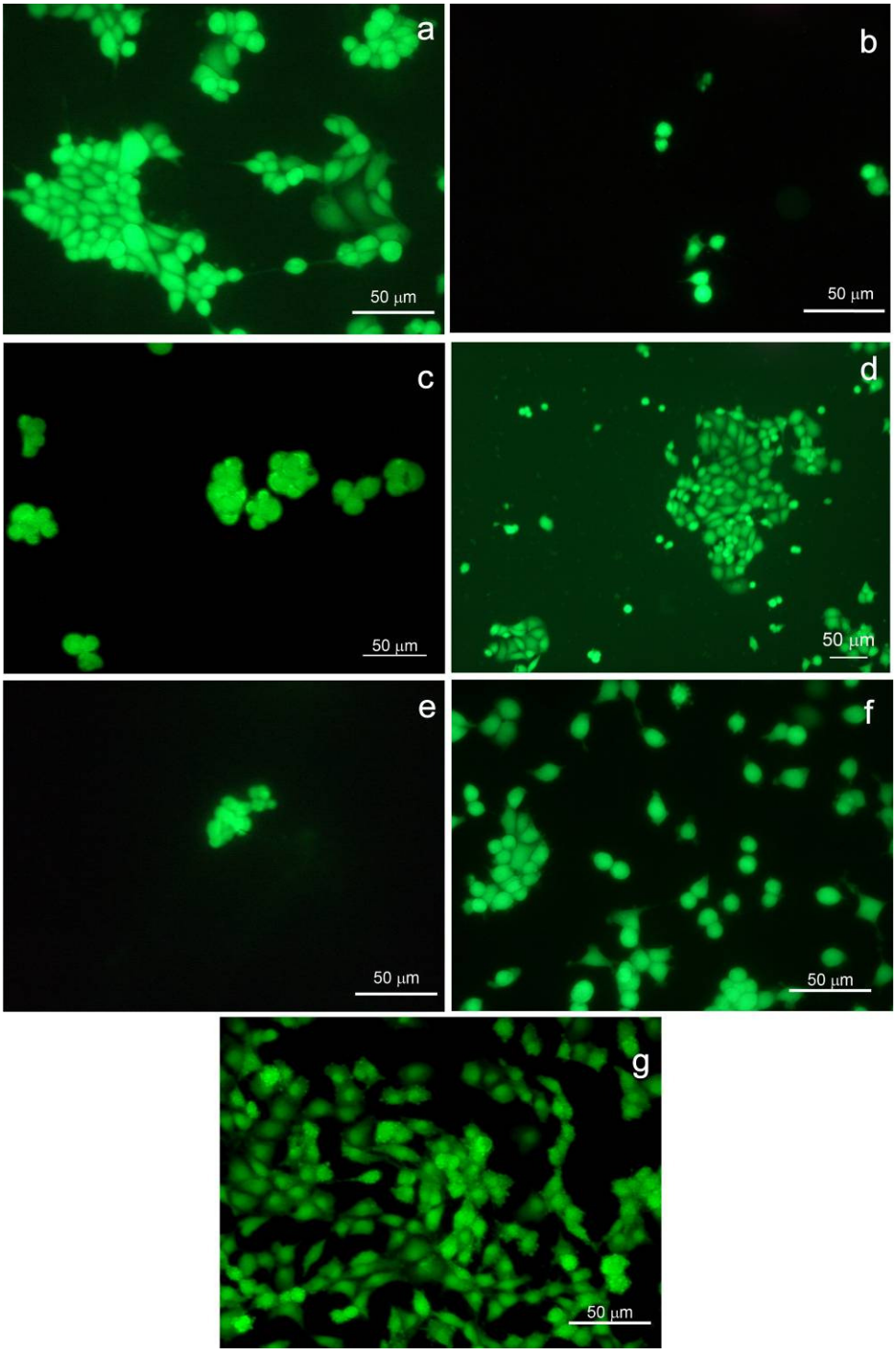

Figure 2.4 – Fluorescence microscopy images of FDA-stained PC12 cells on 6 different surfaces after 24 hours incubation time. (a) Flat silicon surface, (b) Freshly etched, (c) Oxidised, (d) APTMS silanised, (e) PEG silanised, (f) FBS coated and (g) Collagen coated pSi surface. The cell density estimated from these images were (a) 482 cell/mm^2, (b) 50 cells/mm^2, (c) 120 cells/mm^2, (d) 315 cells/mm^2, (e) 27 cells/mm^2, (f) 342 cells/mm^2 and (g) 535 cells/mm^2.

2.1.2.3 Cell viability assay

XTT assays were performed to a gain a quantitative understanding on how the surface modifications affect cell attachment and viability. This assay measures the formation of orange formazan dye release through cleavage of yellow tetrazolium salt XTT by mitochondrial dehydrogenases in metabolically active cells[34]. Only viable cells can perform this metabolic cleavage and the resultant formazan dye absorbs strongly at 450 nm.

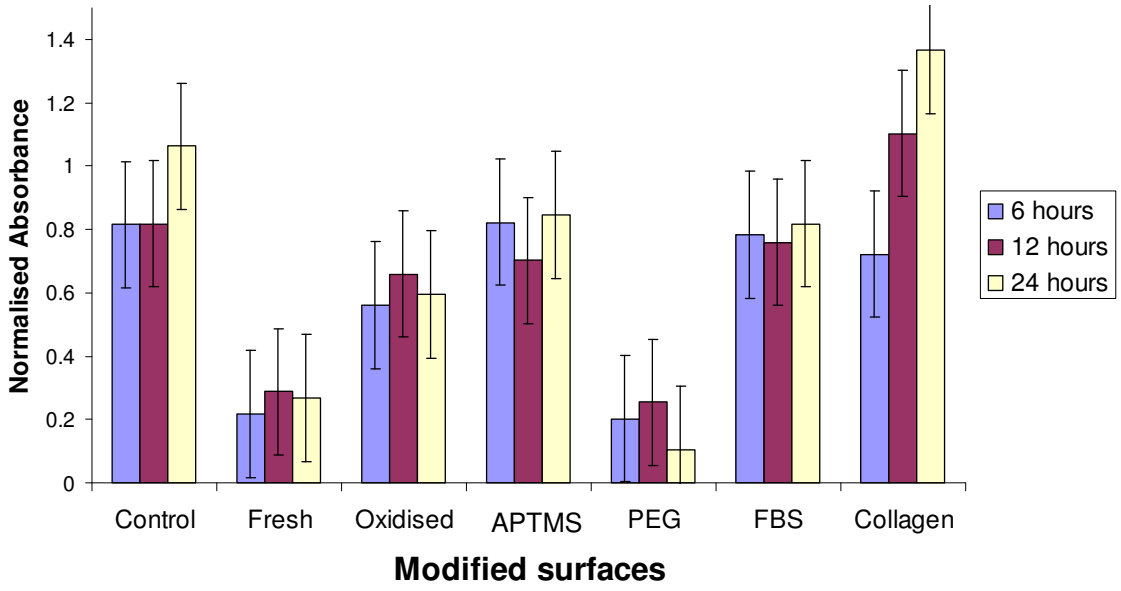

Figure 2.5 – XTT cell viability assays for all modified pSi surfaces after 6, 12 and 24 hours incubation time. All XTT readings were taken in triplicates.

Measurements were taken at the 6, 12 and the 24 hour incubation interval for each of the samples as shown in figure 2.5. At the 6 hour interval, absorbance values were fairly similar for control, APTMS silanised pSi, FBS and collagen coated surfaces. Absorbance values for oxidised surface were slightly lower, while freshly etched and PEG silanised pSi surfaces registered the lowest absorbance values. At the 12 hour culture interval, the absorbance

values for all surfaces remained relatively stable as compared to the 6 hour interval except for the collagen coated surface which had shown a substantial absorbance increase. After 24 hour interval, the oxidised, APTMS silanised pSi and the FBS coated surfaces maintained its absorbance values, fairly similar to those measured at the 6 and 12 hour interval. While PEG silanised pSi showed a reduction in absorbance at the 24 hour interval, both control and collagen coated surface exhibited an increased in their absorbance value.

In summary, we recorded the highest absorbance values for control and collagen coated surfaces. The absorbance values remained fairly constant for the oxidised pSi, APTMS silanised pSi and FBS throughout the 24 hours. The freshly etched and the PEG functionalised surfaces had the lowest absorbance values. While the low absorbance value from the oxidised surfaces was maintained, there was a marked reduction in absorbance by the 24 hour mark on the PEG silanised pSi. This may suggest that while a small number of cells attaching on oxidised surface had managed to retain some vitality, they were compromised over time by the PEG silanised surfaces. On the other hand, cell vitality was seemingly enhanced by the collagen-coated surfaces, as evident by the gradual increase in absorbance over time.

2.1.3 Conclusion

Our experiments demonstrated that it is possible to perform a wide range of surface modifications on pSi with very simple chemistry. By means of silanisation on oxidized pSi, we were able to convalently attached chemical moieties easily onto the surface, while proteins readily adsorbed onto the surface. Furthermore, chemical based modifications had conferred greater stability of the film in the aqueous environment, an important consideration for biological applications of pSi. Stability can also be improved by protein adsorption, as in the case of FBS and collagen coating. Moreover by adsorbing proteins onto the surface, it is possible for us to elucidate interesting cellular behavior on the surface. For example, by functionalising with FBS, cell attachment was encouraged while the development of neuronal processes was observed to be impaired by the presence of both soluble and attached FBS molecules[34]. Adsorption of collagen on the pSi surface encouraged both cell attachment and viability on the surface while PEG functionalisation onto the surface greatly reduced cell attachment. Furthermore XTT assay performed on these PEG surfaces further suggested that the vitality of the cells on these surfaces may have been compromised over time.

2.2 Long term culture and functional characterisation of primary hepatocyte cells on pSi films

The concept of organ replacement from laboratory tissue culture is one of the driving motivations for the numerous researches in the field of biomaterials. Researchers strive to create cell containing scaffold materials that can either serve as replacements or alternatives to the damaged organs within the body[35-37]. For this purpose, hepatocytes and neurons have already been extensively used in current literature with intention to ultimately produce workable artificial livers[17, 35, 38] or neuronal networks[39, 40] *in vitro*.

There are many factors to consider in this endeavour. One of the most important challenges is the long term maintenance of tissue viability *in vitro* and is often deemed as one of the most crucial issues in biomaterial application[18, 38, 41]. To achieve long term maintenance of tissue culture, researchers have often tried to mimic conditions similar to those found *in vivo*. The choice of biomaterial used for the scaffold or support for the long term culture is therefore the critical factor.

In the previous section, the versatile nature of pSi as a biomaterial was highlighted by introducing a variety of changes to the surface chemistry and the effects on cell attachments arising from these changes were investigated. We showed that by means of surface modifications, it is possible to control the cellular morphology and vitality on pSi surfaces. The tunable nature of chemistry on pSi surface is an important feature when designing biomaterials. This is because for long term maintenance of cell culture, surface modification of the support material is often deemed necessary[16, 17, 38].

To gain a better understanding of the suitability of pSi as a biomaterial, we decided to perform a long term cell culture study. Apart from chemical modifications as discussed earlier, it is also important to understand how physical cues may influence cellular behavior. Thus, in order to address these issues, pSi surfaces of different pore sizes were fabricated and a variety of surface modifications was performed on these surfaces. Primary hepatocytes were seeded on these surfaces and incubated over a course of 2 weeks. Cell morphology of the primary hepatocyte on the different surfaces was subsequently studied by confocal microscopy while the production of urea and lactate dehydrogenase enzyme were also measured to quantify the metabolic activity and viability of the hepatocyte over the course of the 2 weeks.

2.2.1 Materials and methods

2.2.1.1 Etching procedure

pSi samples were prepared from p-type (boron-doped) silicon wafers with (100) orientation and resistivity of 0.0005-0.001Ω·cm (**Virginia Semiconductors**). Samples were etched in a 3:1 (v/v) solution of 49% aqueous HF/EtOH at 4 constant current densities of 28.3 mA/cm^2, 56.6 mA/cm^2, 113.18 mA/cm^2 and 226.37 mA/cm^2 at 120s, 60s, 30s and 15s, respectively. The freshly etched pSi surfaces were then rinsed with methanol, acetone and dichloromethane and were dried under a stream of N_2. The surfaces were subsequently oxidised thermally at 600º for 1 hour in the furnace (Labec HTF50/12 1200°C Tube Furnace). After the thermal oxidisation, the pSi surface was cut to 10 mm^2 pieces with a diamond scribe.

2.2.1.2 Atomic force microscopy

Atomic force microscopy (AFM) images of pSi were acquired on a Nanoscope IV Multimode microscope (Veeco Corp.) operating in tapping mode using silicon tips (FESP, Digital instruments) with a resonance frequency of 50-70 kHz. Nanoscope III v5.30r3 software was used to perform offline analysis of the images

2.2.1.3 Surface modifications

Three different surface modifications were used on the pSi surfaces of four different pore sizes: Oxidised, APTMS silanised, collagen coated. Round tissue culture polystyrene disk (TCPS) with a surface area of 13 mm^2 were also used as controls.

The functionalisation of APTMS was as described in section 2.1.1.2. For the collagen coated surfaces, 10 µg in 10 ml 0.1M acetic acid of Type I rat collagen was prepared and applied dropwise onto thermally oxidised pSi surface and was incubated for 1 hour. After the incubation, the surface was gently rinsed twice with filter-sterilised 1X PBS.

2.2.1.4 Collagen sandwich system

For the collagen sandwich system, the surfaces were first coated with collagen as described above. A collagen gel was prepared by adding 10 µl of 10X DMEM to 90 µl of collagen (10 µg in 10 mls 0.1 M acetic acid) and was placed on ice to avoid solidification at room temperature[42]. The primary hepatocytes were seeded firstly onto the surface and incubated for 4 hours. The culture media was then removed from the wells and the cold gel was gently added dropwise with a sterilised Pasteur pipette onto the pSi surface. 10 mins of incubation at room temperature was allowed for the gel to set on the surface before fresh media was added into the culture wells. The collagen sandwich gel was applied on all collagen coated surfaces (TCPS and pSi).

2.2.1.5 Isolation of the primary hepatocytes

Approval for all animal studies was obtained by the institutional animal ethics committee. Hooded Wistar rats were first sedated in the fume hood with Fluothane (**Parnell Laboratories (AUST) Pty.Ltd**) and anaesthetised immediately via intraperitoneal injecting with a cocktail combination of ketamine (**Parnell Laboratories (AUST) Pty.Ltd**) and xylazine (**Troy Laboratories Pty.Ltd**). The liver (approximately 9 grams) was subsequently removed and processed into a soupy mixture using scissors on ice. The tissue was then washed with serum free balanced silane solution (BSS) buffer containing 0.225 g/l of glucose, 0.6 g/l of bovine serum albumin (**Cohn fraction V, Cat#1328A, Research Organics**), 0.00125 g/l of $MgSO_4.7H_2O$, 1% vol/vol $CaCl_2$ and 50 µg/ml of 1:1 penicillin (**Sigma, Cat #P-3032**) and streptomycin (**GibcoBRL**) and adjusted to a pH of 7.2. 100ml of this wash buffer was added to the mixture and was subsequently gauze filtered. The filtered solution was then centrifuged at 500 rpm for 75 seconds and the supernatant was carefully decanted. The pellet was resuspended with ice-cold wash buffer and centrifuged again. The supernatant was then removed and the pellet was weighted out. The pellet was finally resuspended with 50 mls of DMEM and was kept on ice before use.

2.2.1.6 Primary hepatocyte culture on pSi

The 1 cm^2 pSi surfaces were placed aseptically in 12-well plates in the laminar flowhood and 200µl of the primary hepatocyte with a density of 3.7 x 10^5 cells/ml were seeded on each of these surfaces. 980 µl of filter sterilised 1:1 HAM F12:DMEM (**Invitrogen**) attachment media with 50 IU/ml penicillin/streptomycin and supplemented with both 10 µl of

dexamethasone (1 mg/ml in 5% EtOH) and 10 µl of insulin (5 mg/ml) was added to the cells and was incubated for 4 hours. After the 4 hours incubation time, the surfaces were carefully removed from the wells and rinsed with sterilised 1X PBS to remove unattached cells. The surfaces were then transferred to new 12 well plate and 2 mls of 1:1 HAM F12:DMEM supplemented with 5 % FBS, 10 µl of insulin (5 mg/ml) and 50 IU/ml penicillin/streptomycin was added to the cells. The wells were incubated at 37°C for 2 weeks. The media from the wells were collected and replaced with fresh media every 2 days while the collected media were stored in a -80ºC freezer. All cell culture on the surfaces was performed in triplicates.

2.2.1.7 Laser scanning confocal microscopy

Confocal microscopy was performed using a Leica TCS SP5 laser scanning confocal microscope after an incubation time of 2 and 14 days. At the end of the incubation time, the cells were incubated with 2 µg/ml of Hoechst 33342 dye for 30 mins before gently rinsing the wells twice with 1X PBS (0.014 mM NaCl, 0.27 mM KCl, 0.8 mM Na_2HPO_4 and 0.8 mM KH_2PO_4 and adjusted to pH 7.4). The cells were subsequently fixed with 3.7% formaldehyde in 1X PBS for 10 mins at room temperature and washed with PBS. After fixation, 5mls of 0.1% Triton X-100 in PBS was added to each well for 5 mins and each well was rinsed again with PBS. 5 µl of 6.6 µM of Alexa Fluor® 594 phalloidin (**Invitrogen**) was added to 200 µl of PBS and the solution was added into each well and incubated in the dark for 30 mins. The cells were finally rinsed with PBS and stored in 10 % glycerol in PBS and adjusted to pH 8.0 (buffered glycerol) in the dark. Confocal microscopy was then performed.

2.2.1.8 Urea and lactate dehydrogenase assay

Urea produced by the cells was analysed every 2 days using a **Wako** Urea N B diagnostic kit. In brief, the urease was first dissolved with glycerin and this solution was diluted 20 fold with phosphate buffer containing sodium silicylate and sodium pentacyanonitrosyl ferrate (III) dehydrate as provided by the supplier. 400 µl of this diluted urease solution was then added with 400 µl of a solution of sodium hypochlorite and sodium chloride provided by the supplier. 4 µl of the culture media that were collected every 2 days was added to this mixture and thoroughly mixed before incubating at 37º for 15 mins. After the incubation, the absorbance value was determined on a Hewlett Packard 8452A diode array spectrophotometer and analysed using Agilent 8452 UV-Visible Chemstation Software at the absorbance wavelength of 570 nm.

Lactate dehydrogenase (LDH) assays were performed by first adding 30 µl of the collected culture media to 100 µl of 1 mM NADH and 10 µl of 20 mM pyruvate and thoroughly vortexing. Subsequently, the mixture was then transferred to sample cups purchased from **Roche** and was analysed with the COBAS FARA Centrifugal Analyser at an absorbance wavelength of 340 nm.

2.2.2 Results and Discussion

2.2.2.1 AFM analysis of the pSi surfaces

The size of pores attainable for electrochemical anodisation of silicon is dependent on many factors and one of them is resistivity. The wafers used in this section were highly doped p++ silicon with lower resisitivity (0.0005-0.001Ω·cm) as compared to the wafers used in the previous section (3-6 Ω·cm). This change in wafer resistivity was motivated primarily by the fact that the variation in pore range attainable from wafers with lower resistivity is much larger[7, 43] than those attainable from higher resistivity silicon[9]. In order to gain a better understanding of how pore size can influence cell attachment and morphology, it was necessary to produce a wider variation of pore sizes on the surface.

Highly doped pSi surfaces were prepared under 4 different anodisation currents, 28.3 mA/cm^2, 56.6 mA/cm^2, 113.18 mA/cm^2 and 226.37 mA/cm^2. These different anodisation currents produced surfaces with different pore sizes and the anodisation time for all the 4 pSi surfaces were also adjusted to keep a constant charge at appromixately 3396 coulombs/cm^2 in order to maintain a consistent film thickness. After the anodisation, AFM was performed on these surfaces to determine the average pore sizes. Representative AFM images are shown in figure 2.6.

The average pore size for 28.3 mA/cm^2 current density was found to be 8 nm (figure 2.6 (a)) while doubling the current density to 56.6 mA/cm^2 produced an average pore size of 14 nm (figure 2.6 (b)). When the current density was doubled again to 113.18 mA/cm^2, pore sizes

on the pSi surface were found to be approximately 23 nm (figure 2.6 (c)). The highest current density applied in our surface was 226.37 mA/cm^2 and this yield pores of approximately 38 nm wide (figure 2.6 (d)). These findings demonstrates that the size of the surface pores on pSi is controlled by the amount of anodisation current applied, i.e. the larger the anodisation current, the larger the pores[44, 45]. AFM performed on TCPS surfaces also revealed uneven surface features, as shown in figure 2.6 (e).

At lower current density, surface pores were observed to be rounder in shape while the pores were replaced by larger disorganised elongated and canal-like pores found on surfaces anodised at higher current densities (figure 2.6 (d)). This kind of change in pore morphology is not uncommon for highly doped porous silicon[46].

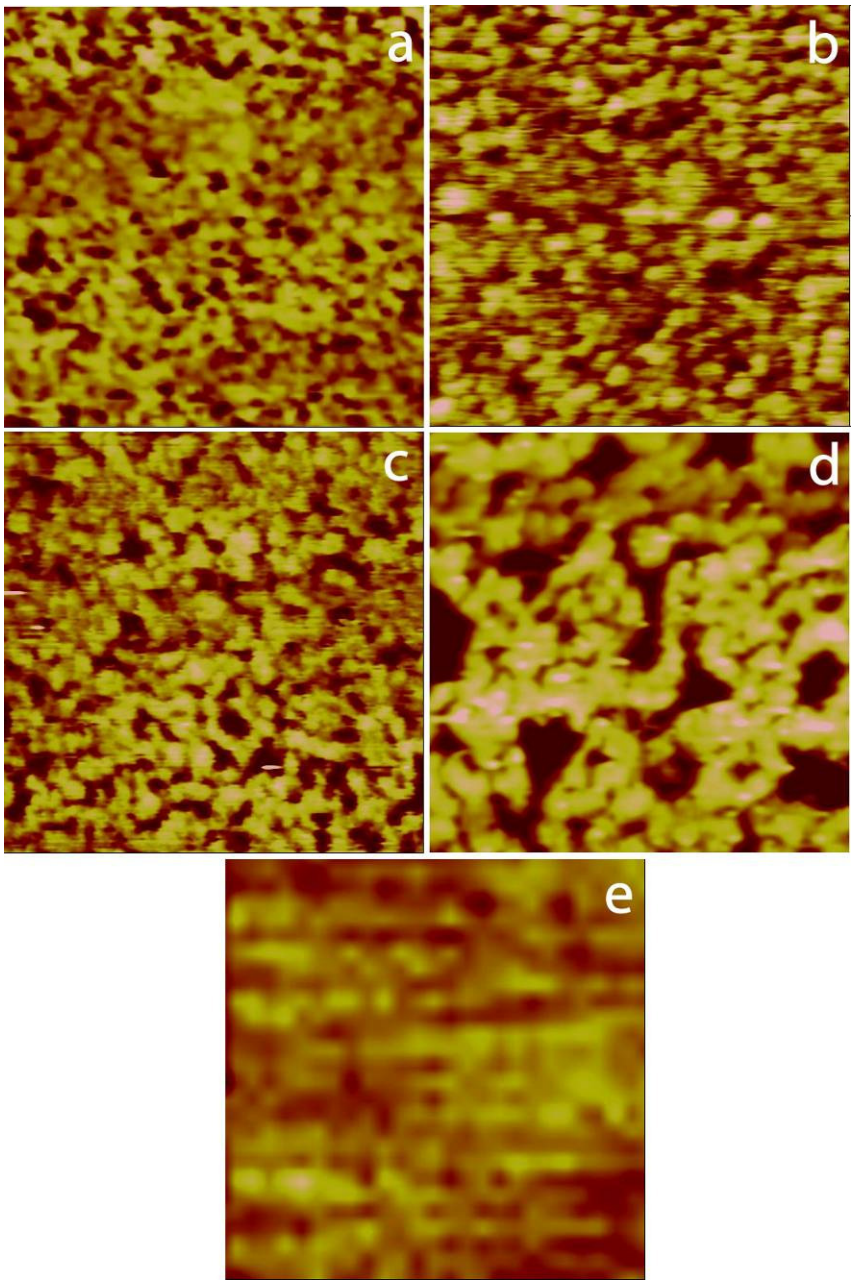

Figure 2.6 – AFM images of pSi surface anodised under the current density of (a) 28.3 mA/cm^2, (b) 56.6 mA/cm^2, (c) 113.18 mA/cm^2 and (d) 226.37 mA/cm^2. (e) Shows the AFM image of the TCPS surface. All images are of a 200 nm size. The z-scale of (a), (b), (c) and (e) are 5 nm while (d) is 10 nm.

2.2.2.2 Laser confocal scanning microscopy

In the previous section, we demonstrated that APTMS silanisation can promote PC12 attachment on the surface and the results were comparable to unmodified flat silicon. To further investigate the effects of surface modification on long term cell culture, we isolated primary hepatocytes from rats and incubate them on different modified surfaces of different pore sizes. As mentioned in the introduction chapter, collagen is an extra cellular matrix (ECM) protein that can promotes cell adhesion on the surface[47]. Furthermore, by sandwiching hepatocytes between two collagen layers, it has been shown to greatly enhance and maintain cellular viability in long term culture[41, 48, 49]. Thus, in order to perform a study on long term cell viability, we introduced 4 surface modifications on thermally oxidized pSi: APTMS silanised, collagen coating and collagen sandwich. These surface modifications were applied to samples with 4 different average pore sizes. These surfaces were then incubated for 14 days. Media renewal was performed every 2 days in order of the maintain the viability of the cells and collected media was used for further LDH and Urea assaying[50, 51]. Cell morphology on these surfaces was studied at the beginning and the end of the experiment time frame, on day 2 and day 14, by means of confocal microscopy after the primary hepatocytes had been stained with hoechst and Alexa Fluor® 594 phalloidin**.**

On surfaces with an average pore size of 8 nm (anodised at 28.3 mA/cm^2), the overall cell morphology on oxidised surfaces and APTMS pSi surfaces after 2 days were typically round and the cytoskeleton of these cells were not readily detected from confocal microscopy as shown in figure 2.7 (a) and (b) respectively. Both collagen coated and the collagen sandwich showed high confluency displaying well-spread cytoskeleton maintaining good intracellular contact, as shown 2.7 (c) and (d) respectively. By day 14, we noticed that while there were

still some cells adhering on the oxidised surfaces (figure 2.7 (e), disruption of the cytoskeleton was frequently observed as reflected by the appearance of actin fiber clusters observed on the cell and this is a feature commonly found in cells undergoing apoptosis[52, 53]. This suggested that cells were dying on the oxidised surface after 14 days. Interestingly, cells growing on APTMS, collagen coated and the collagen sandwich surfaces all shared a rather similar morphology at day 14, i.e. showing rounded cells as indicated by a ring of cytoskeletal protein around the cell nucleus (see figure 2.7 (f)-(h))

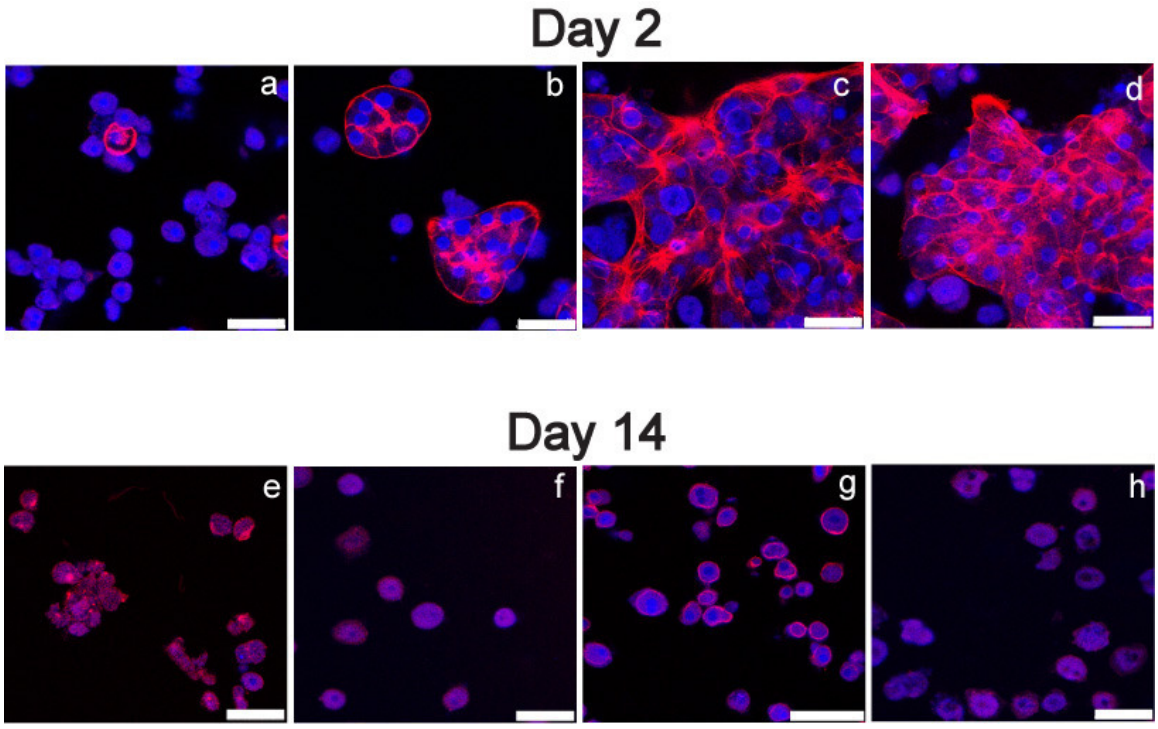

Figure 2.7 – Confocal microscopy images of primary hepatocytes growing on surface modified pSi (pore size = 8 nm) at day 2 and day 14. The surface modifications are as follows: (a) and (e) oxidised, (b) and (f) APTMS silanised, (c) and (g) collagen coated, (d) and (h) collagen sandwiching. White bar represents 50 µm. Cells were stained with hoescht and Alexa Fluor® 594 phalloidin.

After 2 days, the primary hepatocytes growing on oxidised and APTMS pSi surfaces with pore sizes of 14 nm (anodised at 28.3 mA/cm^2) showed similar morphology (figure 2.8 (a) and (b)) when compared to those cultured on the same modified surfaces with pore sizes of 8

nm (figure 2.7 (a) and (b)). However, an observable difference between the two different pore sizes for both oxidised and APTMS surfaces was that cells tended to cluster on the 8 nm pore size samples while this clustering was less obvious on the 14 nm pore size samples. Cells cultured on the surfaces that were collagen coated and the collagen sandwich appeared well-spread and healthy (figure 2.8 (c) and (d)). By day 14, there were very few cells left on the oxidised and the APTMS surfaces and disruption of actin fibers around the periphery of the cell could be observed from the confocal images and this was an indication that the cells may have undergone apoptosis. The cell density was significantly decreased, suggesting that a fraction of the cells have died and detached from the surface. There were more cells found on the collagen coated and the collagen sandwiched surfaces and the general morphology of these cells were rounded (figure 2.8 (g) and (h)). However, the periphery of the cells did not display the similar apoptotic characteristic of those on oxidised and APTMS surface.

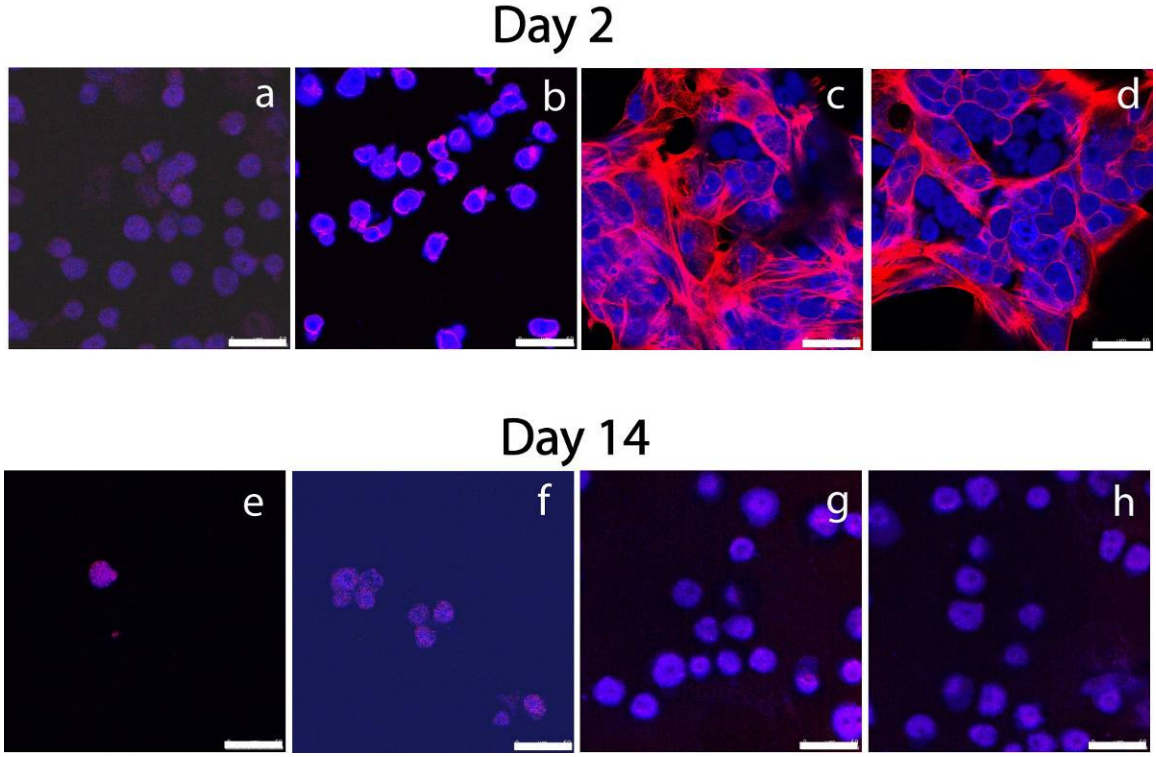

Figure 2.8 – Confocal microscopy images of primary hepatocytes growing on surface modified pSi (pore size = 14 nm) at day 2 and day 14. The surface modifications are as follows: (a) and (e) oxidised, (b) and (f) APTMS silanised, (c) and (g) collagen coated, (d) and (h) collagen sandwiching. White bar represents 50 µm. Cells were stained with hoescht and Alexa Fluor® 594 phalloidin.

On the 23 nm pore surfaces, while there were fewer primary hepatocytes detected on oxidised and APTMS pSi after 2 days compared to the 8 nm and the 14 nm surfaces (figure 2.9 (a) and (b)), cell morphology was also very similar to those 8 nm and 14 nm surfaces. Hepatocytes growing on collagen coated and collagen sandwich surfaces (figure 2.9 (c) and (d)) also shared similar morphological characteristics to those cultured on 8 nm and 14 nm pore surfaces with the same surface modifications at day 2. By day 14, we were only able to detect some cell debris, not intact cells on oxidised surfaces (figure 2.9 (e) while the very few cells detected on APTMS surfaces also shown signs of apoptosis from the cytoskeleton disruption observed in the confocal images along the periphery of the hepatocytes (figure 2.9 (f)). On the collagen coated and the collagen sandwich surfaces, there were many hepatocytes still found attaching to the surface (figure 2.9 (g) and (h)). However, there was one interesting observation made from the collagen sandwich surface. Confocal images had revealed that there was some variation in intensity of the cell nucleus, which could only suggest that the hepatocyte were stacked over one another (figure 2.9 (h)).

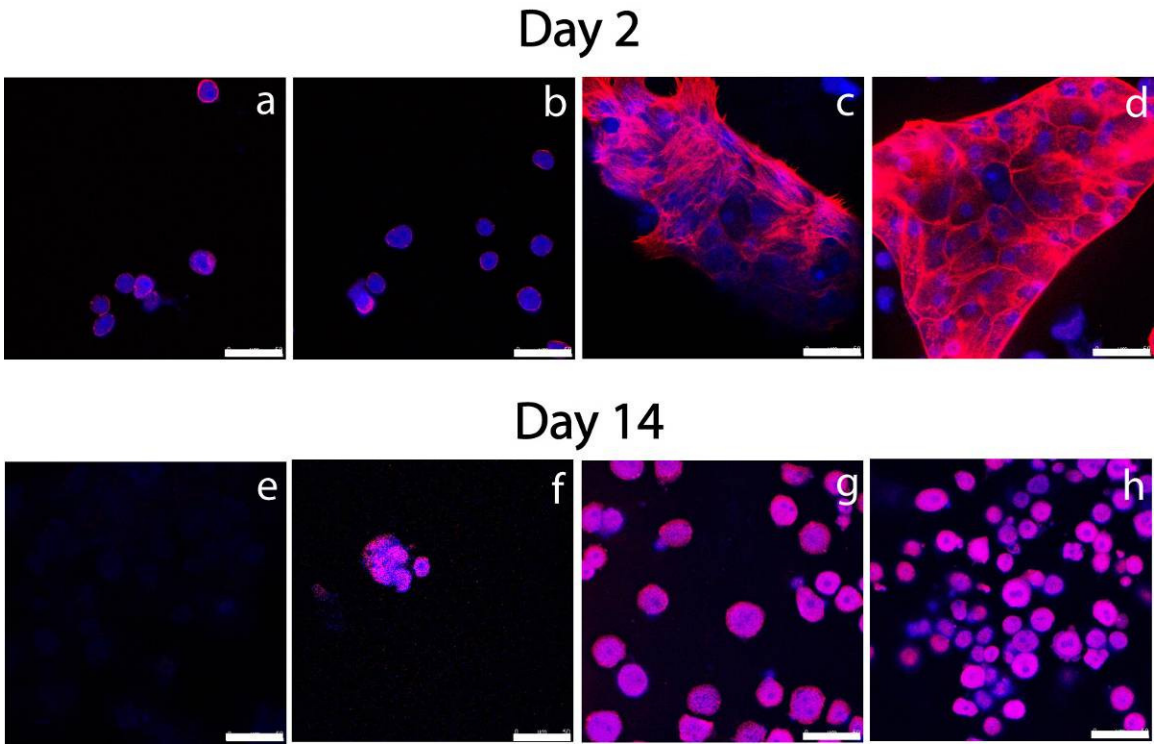

Figure 2.9 – Confocal microscopy images of primary hepatocytes growing on surface modified pSi (pore size = 23 nm) at day 2 and day 14. The surface modifications are as follows: (a) and (e) oxidised, (b) and (f) APTMS silanised, (c) and (g) collagen coated, (d) and (h) collagen sandwiching. White bar represents 50 µm. Cells were stained with hoescht and Alexa Fluor® 594 phalloidin.

For the samples with the largest average pore size (38 nm), hepatocytes on the oxidised and the APTMS surfaces were round in appearance after 2 days of culture (see figure 2.10 (a) and (b)). Yet, early signs of cytoskeletal disruption were evidenced from the disorganised actin fiber observed from those cells attaching on the oxidised surface. Signs of cell stacking were also clearly evident by the different planes displayed from the cytoskeleton and the nucleus of hepatocytes growing on the collagen coated and the collagen sandwich surfaces (figure 2.10 (c) and (d)). On collagen sandwich surfaces, the location of cytoskeleton and nucleus staining strongly suggested that presence of the different planes of attachment. After 14 days of incubation, few hepatocytes could be observed on both oxidised and APTMS surface (figure 2.10 (e) and (f)), while the hepatocytes attaching on the collagen coated and the collagen sandwich had once again shown obvious signs of cell stacking (figure 2.10 (g) and (h)).

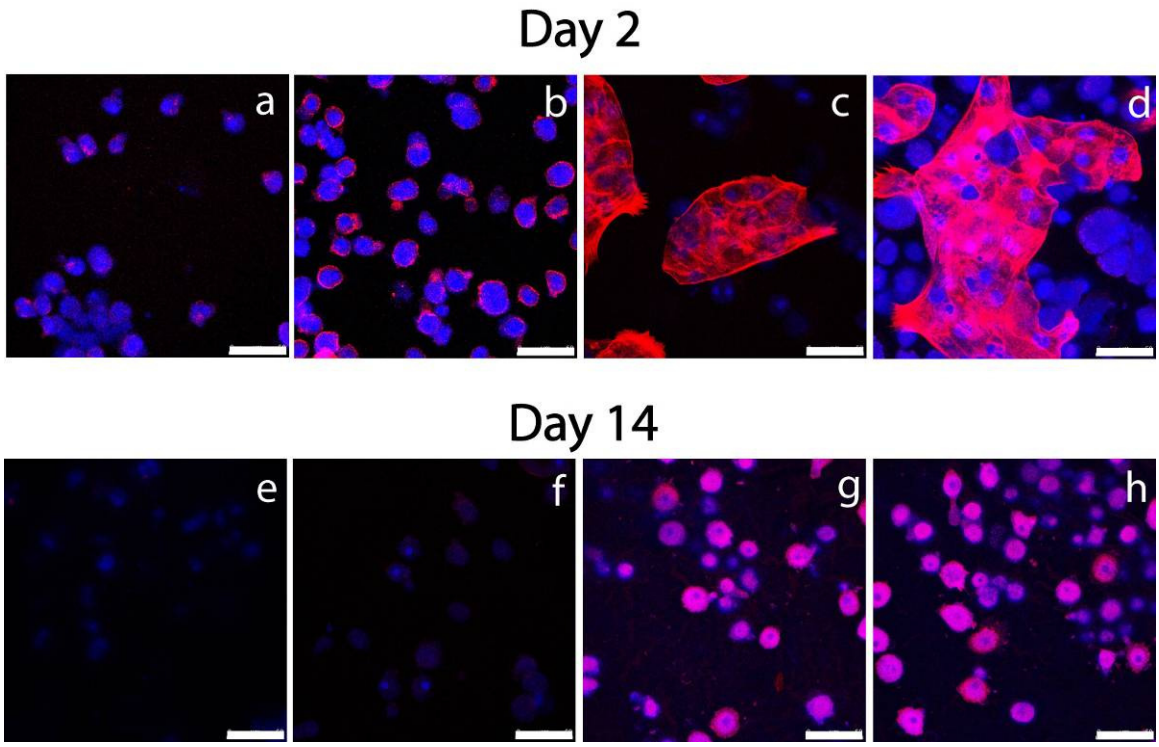

Figure 2.10 – Confocal images of primary hepatocytes growing on surface modified pSi (pore size = 38 nm) at day 2 and day 14. The surface modifications are as follows: (a) and (e) oxidised, (b) and (f) APTMS silanised, (c) and (g) collagen coated, (d) and (h) collagen sandwiching. White bar represents 50 µm. Cells were stained with hoescht and Alexa Fluor® 594 phalloidin.

Cells culture on surface-modified flat silicon surfaces (figure 2.11(a)-(d)) showed good cell spreading and extensive actin fibers at day 2 for all the surface modifications. We also noticed that the hepatocytes found within the collagen sandwich on the flat were higher in number and more densely packed as compared to those cultured within the collagen sandwich on pSi surfaces. Images after day 14 showed the cell apoptosis signs also observed on pSi, on the oxidised and the APTMS flat silicon surfaces (figure 2.11 (d) and (e)). Cells found on both collagen coated and collagen sandwich surface (figure 2.11 (f) and (g)) also displayed the same rounded morphology also observed on all pSi surfaces having the same surface modification by day 14 with a ring of actin fibers surrounding the nucleus.

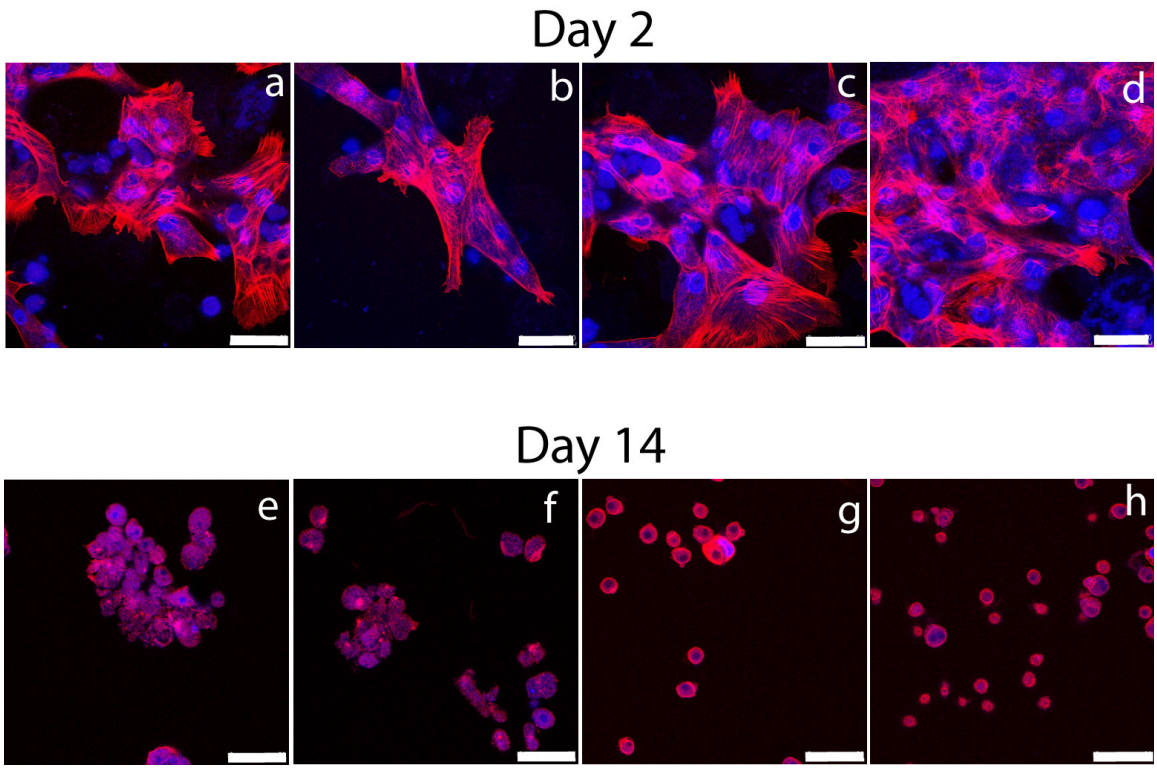

Figure 2.11 – Confocal microscopy images of primary hepatocytes growing on surface modified flat silicon at day 2 and day 14. The surface modifications are as follows: (a) and (e) oxidised, (b) and (f) APTMS silanised, (c) and (g) collagen coated, (d) and (h) collagen sandwiching. White bar represents 50 µm. Cells were stained with hoescht and Alexa Fluor® 594 phalloidin.

Confocal microscopy was also carried out on cells attaching on TCPS surfaces. As shown in figure 2.12, cells were well spread after 2 days and their actin fibers could be easily resolved on unmodified (figure 2.12 (a)), collagen coated (figure 2.12(b)) and the collagen sandwich (figure 2.12 (c)) TCPS. However, by day 14, cytoskeleton extensions from the hepatocytes on the surface were absent and the morphology were generally rounded (figure 2.12 (d)-(f)). After 14 days of culture, there were more hepatocytes observed on all TCPS surfaces when compared to those cultured on pSi surfaces and this may be due to the fact that TCPS surfaces were much flatter and the effects of surface topography has a lesser effect on the residing cells.

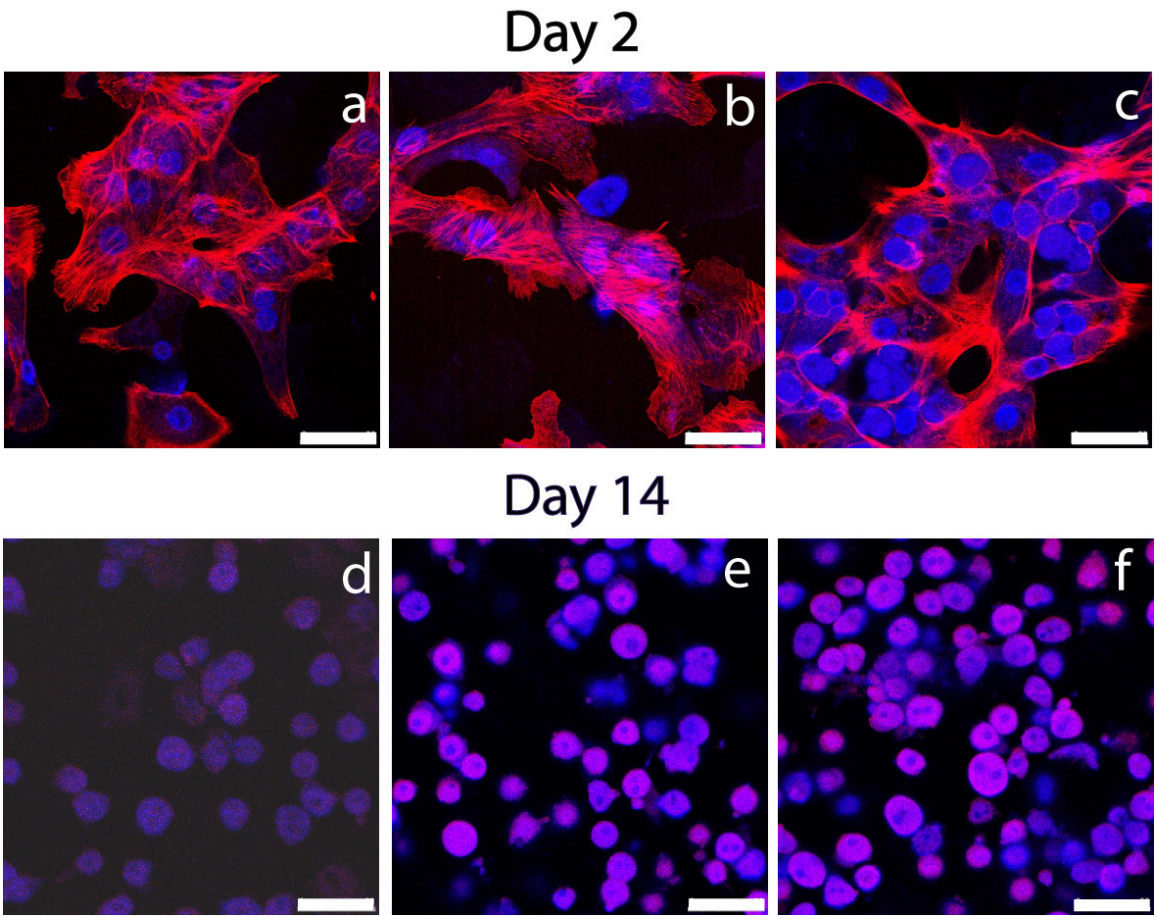

Figure 2.12 – Confocal microscopy images of primary hepatocytes growing on TCPS at day 2 and day 14. The surface modifications are as follows: (a) and (d) unmodified, (b) and (e) collagen coated, (c) and (f) collagen sandwich. White bar represents 50 µm. Cells were stained with hoescht and Alexa Fluor® 594 phalloidin.

In order to visualise hepatocyte stacking on 38 nm pore surfaces that were collagen coated, a 3-dimensional reconstruction on a collagen sandwich surface was calculated from 40 planes at 1.3 µm intervals and is as shown in figure 2.13. The white arrow in the figure shows a specific position whereby 2 different hepatocyte nuclei were observed stacking over each other as the images move down into the z plane. This in turn, confirmed that cell stacking was present on pSi surfaces with pore size of 38 nm and modified with both collagen and collagen sandwich.

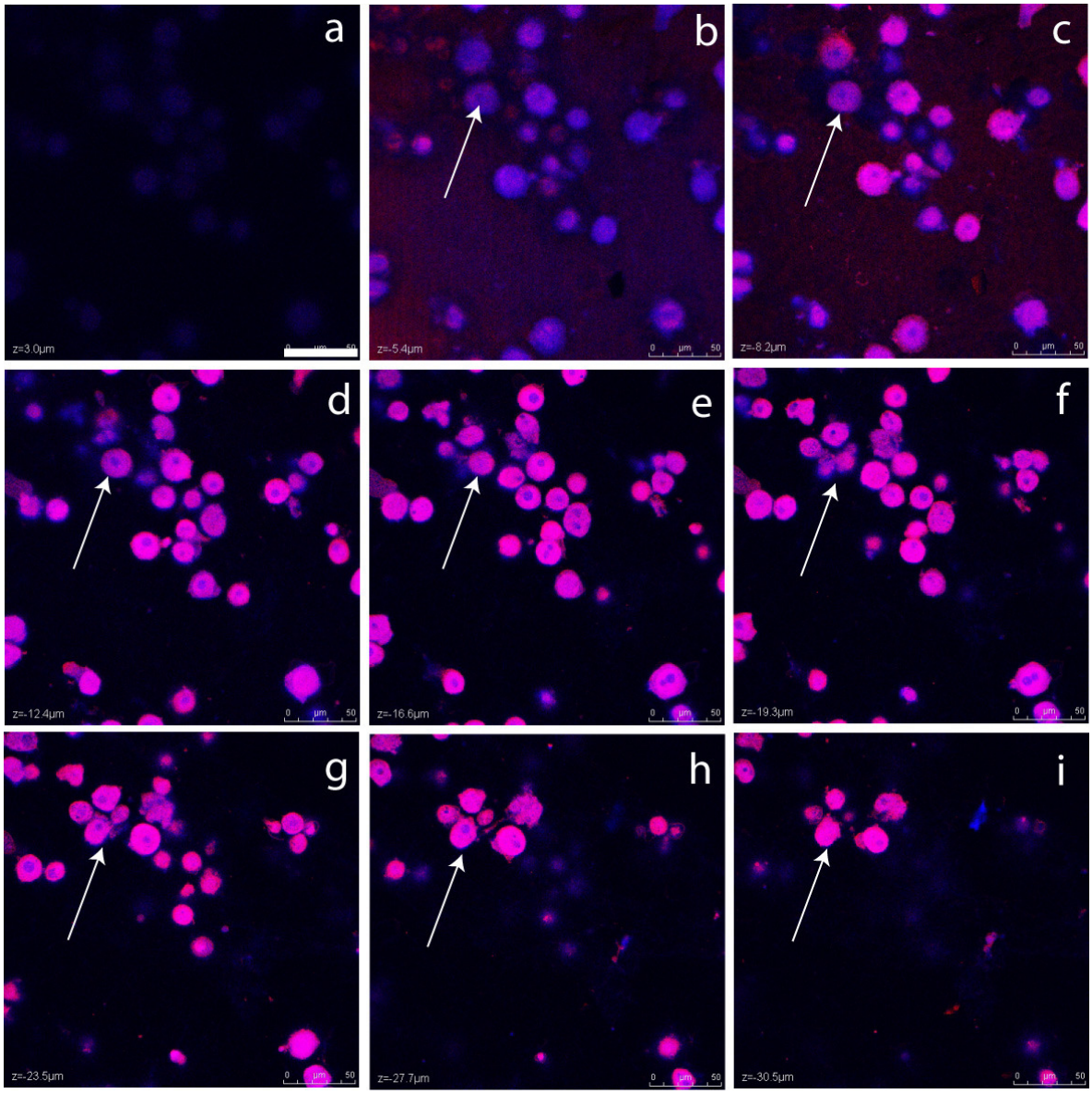

Figure 2.13 – Laser scanning confocal microscopy images taken at different z planes (z stack) of collagen coated pSi film with pore size of 38 nm in 1.3 µm intervals; (a) 0 µm, (b) 2.6 µm, (c) 5.2 µm (d) 9.1 µm, (e) 15.6 µm, (f) 18.2 µm, (g) 22.1 µm and (h) 27.3 µm, from the top from the pSi surface. The arrow as denoted shows a specific position whereby 2 different hepatocyte nucleus were stacked over each other as the images move through the different z planes. The white bar represents 50 µm. Cells were stained with hoechst and Alexa Fluor® 594 phalloidin.

A few conclusions could be drawn from this series of confocal images. Firstly, oxidised surfaces were found not suitable for long term hepatocyte cultures. APTMS fared slightly better than the oxidised surfaces over 2 days, but were also unable to maintain cell attachment after 2 weeks. Cells cultured on oxidised and APTMS surfaces with the smallest pore sizes

(8 nm) tended to form clusters, while cells did not cluster on samples with pore sizes 14 nm and above. We also noticed that on collagen coated and collagen sandwich surfaces, there was a lack of cytoskeleton extension after 14 days of culture. We also observed cell stacking on surfaces with pore size of 23 nm and 38 nm that were coated with collagen or collagen sandwich while the 8 nm and the 14 nm either with collagen coating and collagen sandwich did not show any sign of cell stacking. This suggested that collagen coated surfaces in conjunction with the specific pore region (23-38 nm) may aid in the formation of cell stacks and such cell stacks can have a positive effect on the overall long-term well-being of the primary hepatocytes.

2.2.2.3 Urea and LDH assay

Urea secretion is one of the main indicators for healthy and metabolically active hepatocytes and the quantification of urea production can be used as a measure of viability for the hepatocytes attaching on the different pSi surface[54, 55]. In order to follow hepatocyte viability on our surfaces over the course of 14 days, the amount of urea released from the cells into the media was measured every second day throughout the incubation period.

Figure 2.14 shows the amount of urea released after 2 and 4 days of incubation on the surfaces. At day 2, the concentration of urea detected for hepatocytes growing on the flat silicon surface was found to be the highest (22.33 ± 14.97 µg/ml) for all surfaces. The amount of urea released by the collagen coated surfaces and APTMS silanised surfaces were relatively similar for all the surface modifications (4-8 µg/ml). We also noticed that hepatocytes growing in the collagen sandwich for the 8 nm and 14 nm surfaces had released lower concentration of urea (4.3 ± 0.2 µg/ml and 8.54 ± 2.32 µg/ml respectively) than compared to the collagen sandwich on the flat surface (23 ± 16 µg/ml). However, the concentration of urea released from the collagen sandwich on the 23 nm (16.75 ± 11.09 µg/ml) and 38 nm (8.71 ± 1.59 µg/ml) surfaces were much higher compared to those on the 8 nm and 14 nm samples. This trend in urea concentration for the sandwich surfaces on 23 nm and 38 nm when compared to the 8 nm and 14 nm surfaces was also detected on Day 4. Interestingly, hepatocytes growing in 38 nm surfaces that were collagen coated had dramatically increased its urea concentration (45.29 ± 17.9 µg/ml) while the urea released from hepatocyte growing on the 8 nm and 14 nm collagen coated surfaces remain low (5.29 ± 1.03 µg/ml and 4.35 ± 1.38 µg/ml respectively). Similarly, there was also an increase in the concentration of urea from the collagen sandwich on these larger pores (23-38 nm) when

compared to those in day 2. By comparing between day 2 and day 4, the data might suggest that the effects of collagen deposition (coating and collagen sandwich) on surfaces with pore sizes of 23-38 nm were more readily felt by the cells and resulted in enhanced metabolical activity. On the contrary, collagen deposition on smaller pores (8-14 nm) surfaces did not appear to have a significant effect on urea production. Urea production from hepatocytes growing from collagen sandwich on flat silicon was significantly lower by day 4 than compared to the day 2, and this may indicate that collagen sandwich may have lost its effectiveness on plain flat silicon after a few days of cell culture.

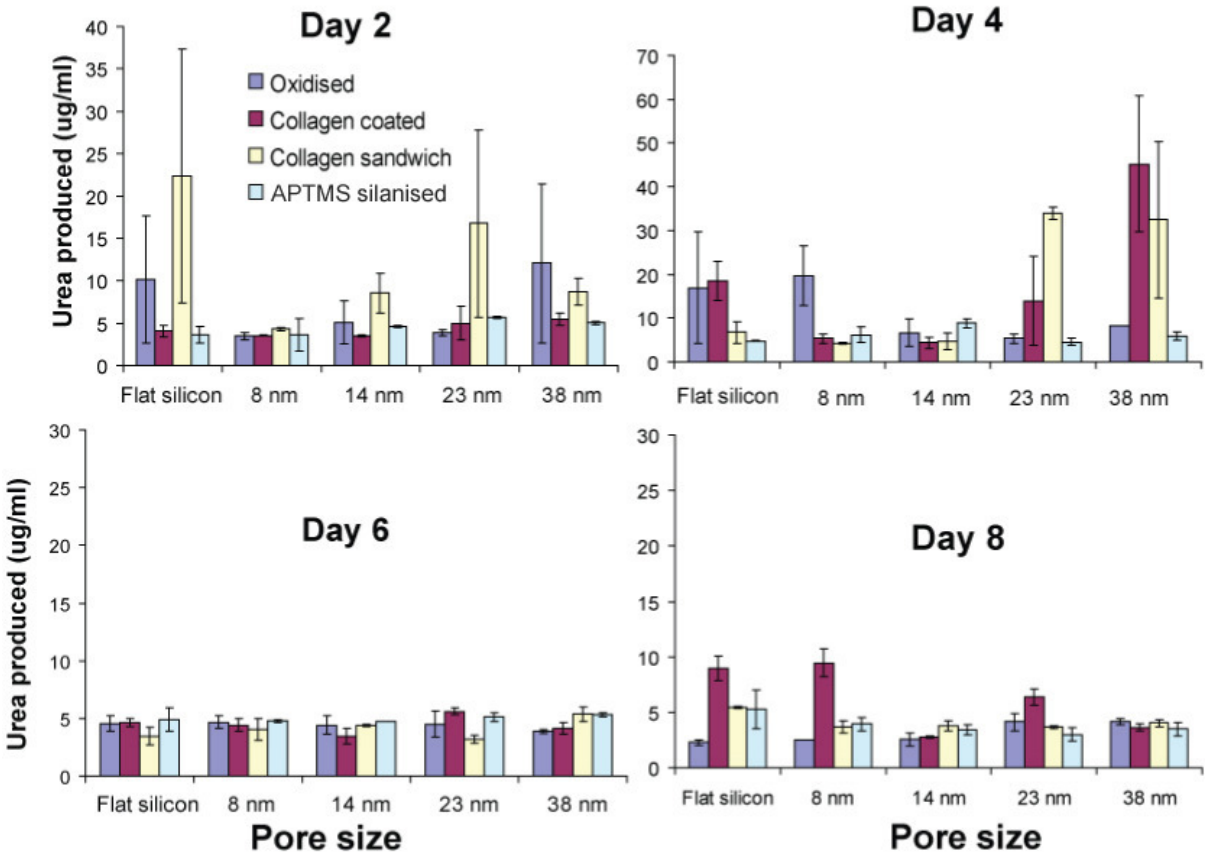

Figure 2.14 – The production of urea from hepatocytes attaching on modified pSi surfaces for day 2, 4, 6 and 8. Urea assays were performed on the supernatant collected at day 2, 4, 6 and 8 with the Wako Urea N B diagnostic kit and samplings were performed in duplicates. The error bars are the standard deviation of the average for the duplicates.

By day 6, we observed that the amount of urea released by the hepatocytes on all different modified surfaces were fairly similar, averaging in the order of approximately 4.5 µg/ml. The concentration of urea produced from cells on the oxidised and the APTMS functionalised surfaces was reduced further by day 8 (see figure 2.14), but we did notice a marked increase in urea production for collagen sandwich on both flat and 8 nm surfaces (8.94 ± 1.12 µg/ml and 9.45 ± 1.25 µg/ml, respectively).

From day 10-14, urea production for surfaces remained low but there was trend of increased urea concentration for all collagen sandwiched surfaces (figure 2.15). From confocal microscopy images taken after 14 days of culture, the presence of cell stacks was earlier shown in section 2.2.2.2 on the collagen coated and collagen sandwich surface. This led us to suspect that the unique stacking behavior of hepatocytes may also be responsible for this maintenance of urea production after 14 days as it has been shown in literature that primary hepatocyte stacking in vitro can aid its viability[36, 49].

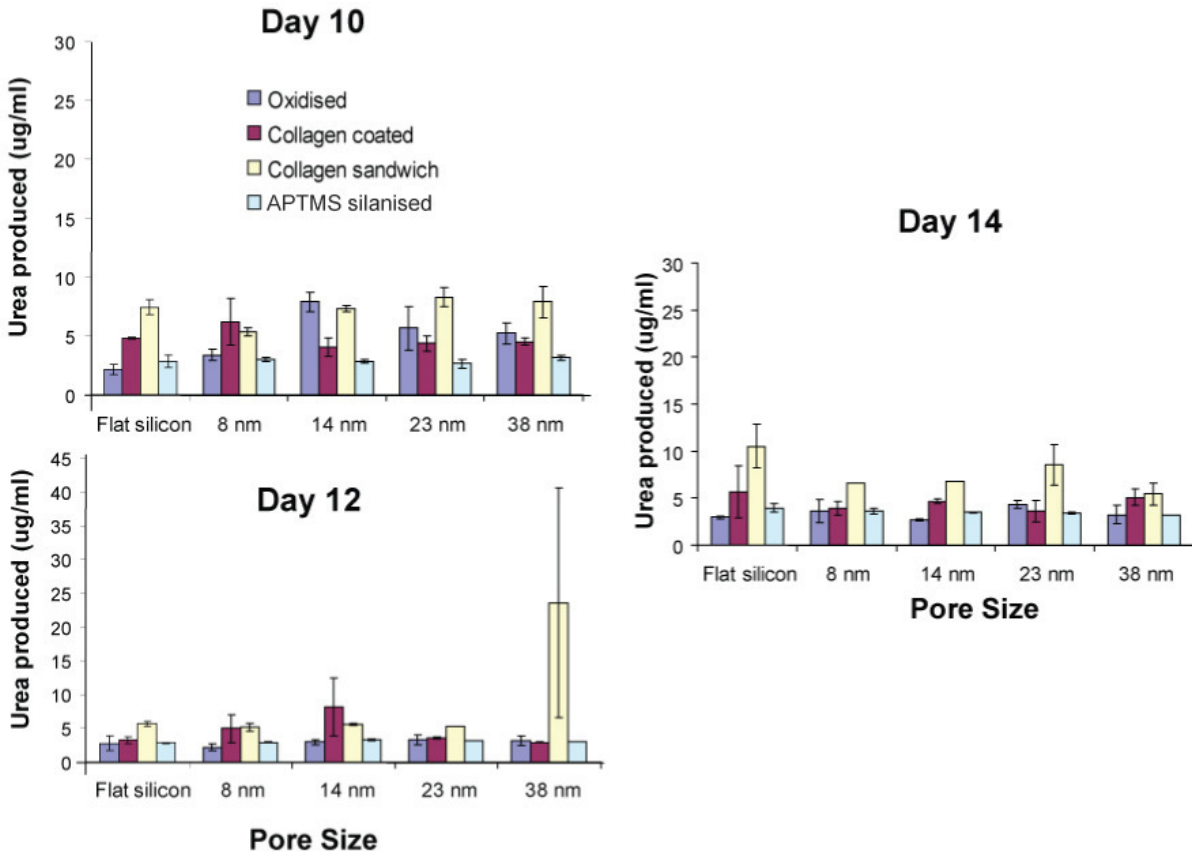

Figure 2.15 – The production of urea from hepatocytes attaching on modified pSi surfaces for day 10,12 and 14. Urea assays were performed on the supernatant collected at day 10, 12 and 14 with the Wako Urea N B diagnostic kit and samplings were performed in duplicates. The error bars are the standard deviation of the average for the duplicates.

The production of urea was also recorded for the TCPS control surfaces. As shown in figure 2.16, on TCPS surfaces, we noticed that day 4 registered a marked increased in urea concentration (38.94 ± 5.84 µg/ml) followed by a rapid reduction in urea production from day 6 to day 14. On the contrary, both collagen coated and collagen sandwich TCPS had maximum urea concentration recorded for day 6 and followed also by a rapid reduction. This reduction in urea production may be caused by massive cell death on the surface and from the data, we hypothesised that collagen coating on TCPS had somewhat delayed the onset of cell apoptosis on the surface when compared to the concentration of urea released on day 6 data from the pSi surface (figure 2.14).

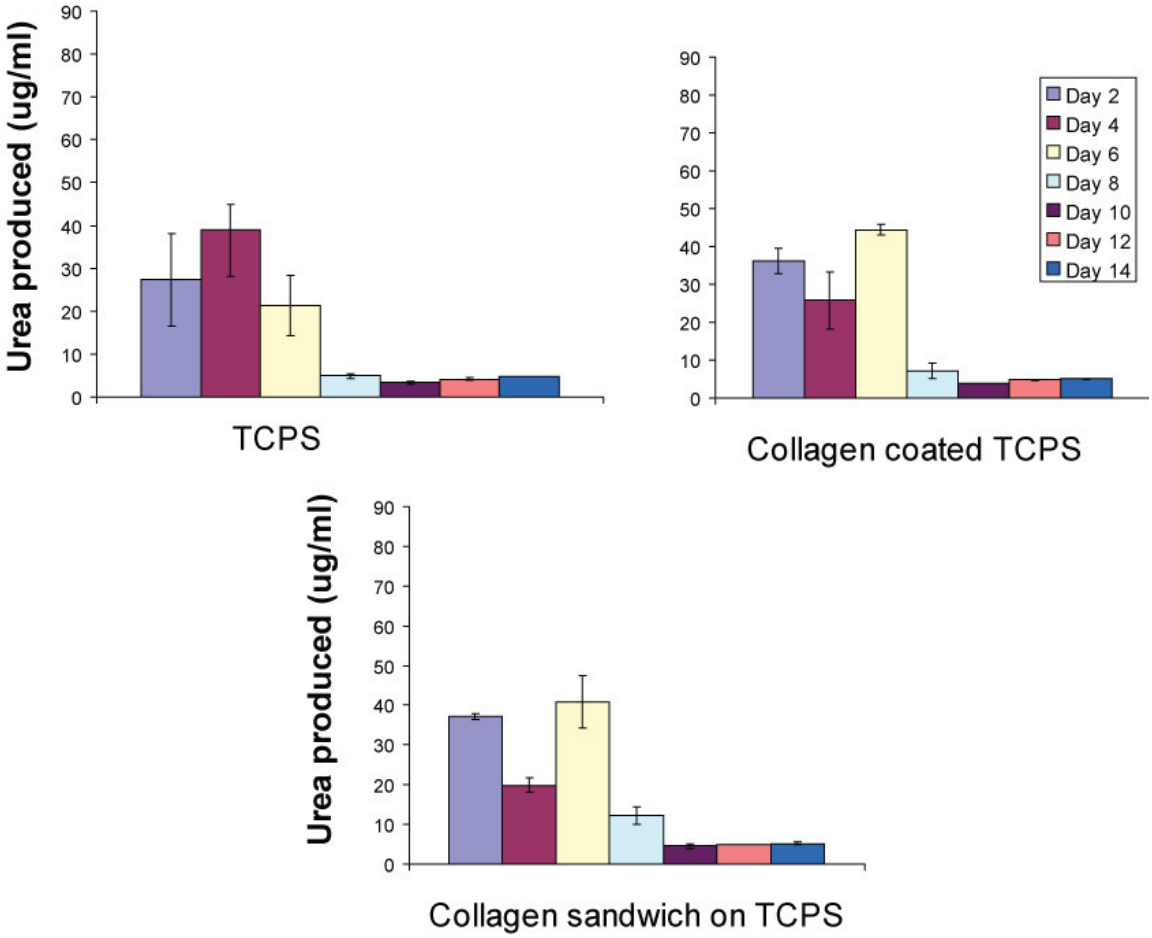

Figure 2.16 – The production of urea from hepatocytes attaching on modified TCPS over 14 days. Urea assay was performed on the supernatant collected that were collected every 2 days with the Wako Urea N B diagnostic kit and all samplings were performed in duplicates. The error bars are the standard deviation of the average for the duplicates.

To correlate the release of urea to the number of viable hepatocytes on the surface, we performed an LDH assay on the media collected every 2 days during the culture period. This assay measures the absorbance of NADH at 340 nm. Upon cell apoptosis, lactate dehydrogenase is released from the dying cells. This enzyme catalyses to the production of lactate from pyruvate and this process converts NADH that is introduced into the media to NAD^+. NADH absorbs strongly at 340 nm, while NAD^+ does not absorb at this wavelength. As such, this NADH absorbance can be used to determine the viability and the extent of apoptosis in the culture.

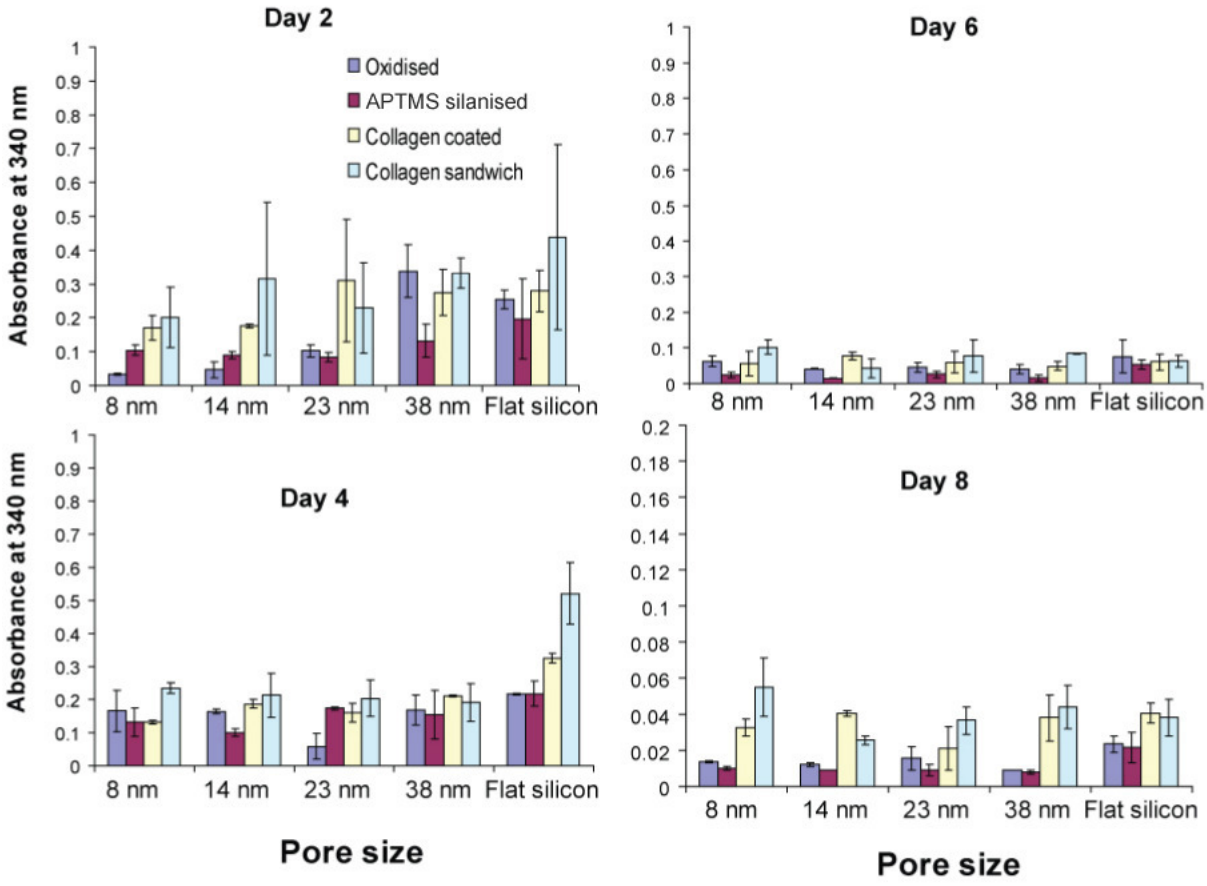

Figure 2.17 – The LDH analysis of hepatocytes attaching on modified pSi surfaces for day 2, 4, 6 and 8. The level of LDH was determined from the media supernatant collected at day 2, 4, 6 and 8 via spectrophotometer measurements at 340 nm. All samples were performed in duplicates. The error bars are the standard deviation of the average for the duplicates.

Figure 2.17 shows the LDH analysis of the hepatocyte from day 2 to day 8 on all modified surfaces. At day 2, media from collagen coated and collagen sandwich generally displayed higher absorbance values as compared to those on the oxidised and APTMS surfaces with the exception of those cultured on plain surfaces. By day 4, collagen coated and collagen sandwich on plain silicon surface also displayed a higher absorbance value (0.613 ± 0.09 and 0.311 ± 0.015) compared to the modified porous surfaces. By day 6 and day 8, absorbance of NADH was found to be low for all surfaces and this suggested extensive hepatocyte apoptosis had already occurred by this stage.

Day 10-14 showed a total reversal in the trend by registering an increase in NADH absorbance for oxidised and APTMS silanised surfaces (figure 2.18). There were also incremental increases observed for the collagen coated and the collagen sandwich surfaces but they were substantially lower than those displayed by the oxidised and the APTMS surfaces. The reason for this reversal in the trend could be explained by our handling protocol. The removal and replenishing of the culture media is deemed necessary for the maintenance of the primary hepatocyte in vitro, as demonstrated in the literature[50, 51]. However, every second day, as the media was being replaced, LDH enzyme was removed from the culture. It is also important to note that by day 14, the absorbance of NADH were still lower than those from the oxidised and the APTMS surfaces and this may suggest that there were still some LDH presence in the media. This could well imply that there may be still cell undergoing apoptosis and we can also conclude that cell viability was maintained for a longer duration by collagen coating and the collagen sandwich setup.

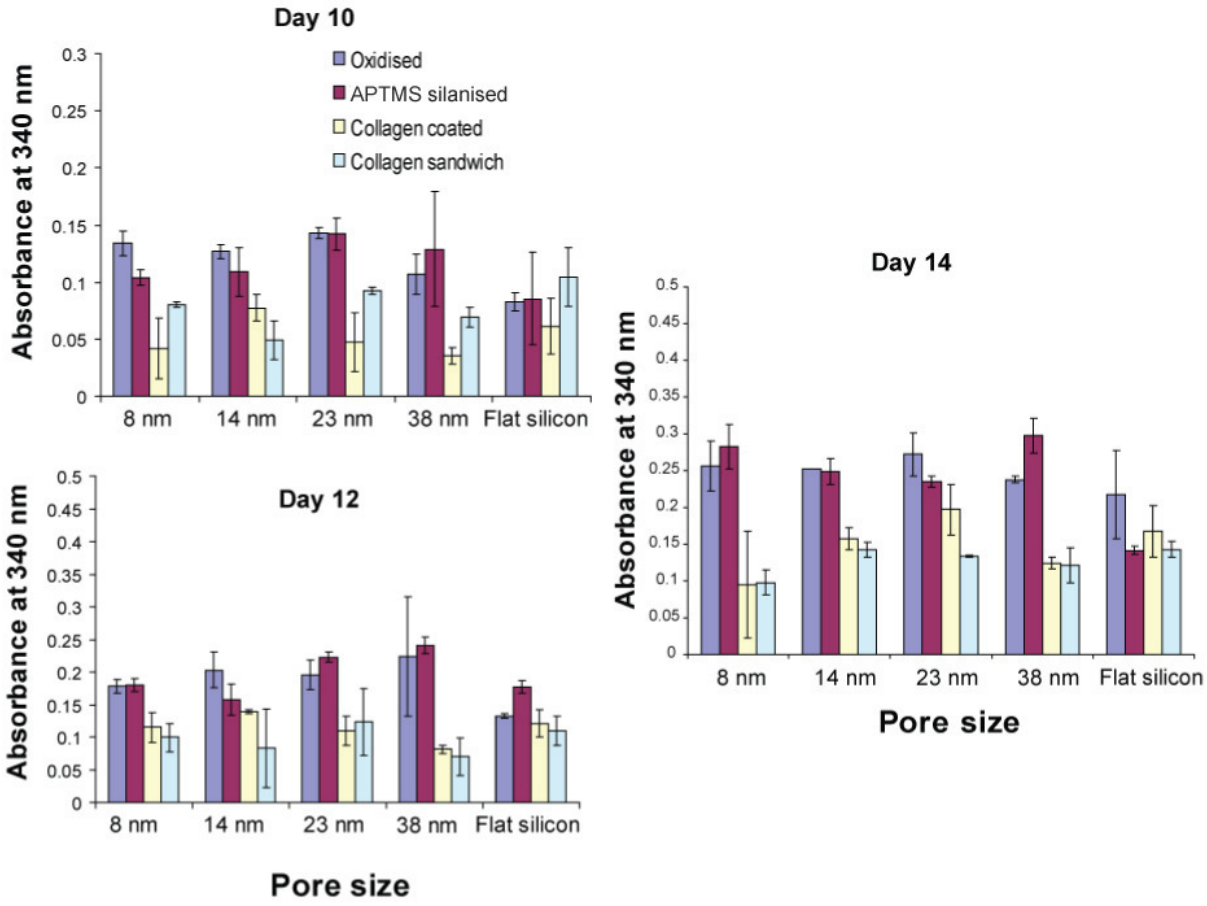

Figure 2.18 – The LDH analysis of hepatocytes attaching on modified pSi surfaces for day 10, 12 and 14. The level of LDH was determined from the media supernatant collected at day 10, 12 and 14 via spectrophotometer measurements at 340 nm. All samples were performed in duplicates. The error bars are the standard deviation of the average for the duplicates.

The maintenance of cells by collagen coating and the collagen sandwich was confirmed by LDH analysis on TCPS surfaces (figure 2.19). Day 2 and Day 4 showed good NADH absorbance which is indicative of good cell viability. The reduction in absorbance was detected from day 6 to day 14 and this suggested that cells had started to die in large numbers by day 6. But more importantly, we notice that by day 14, the absorbance was still fairly low for all the TCPS surfaces and this lead us to conclude that there were still be some cells undergoing apoptosis at this stage.

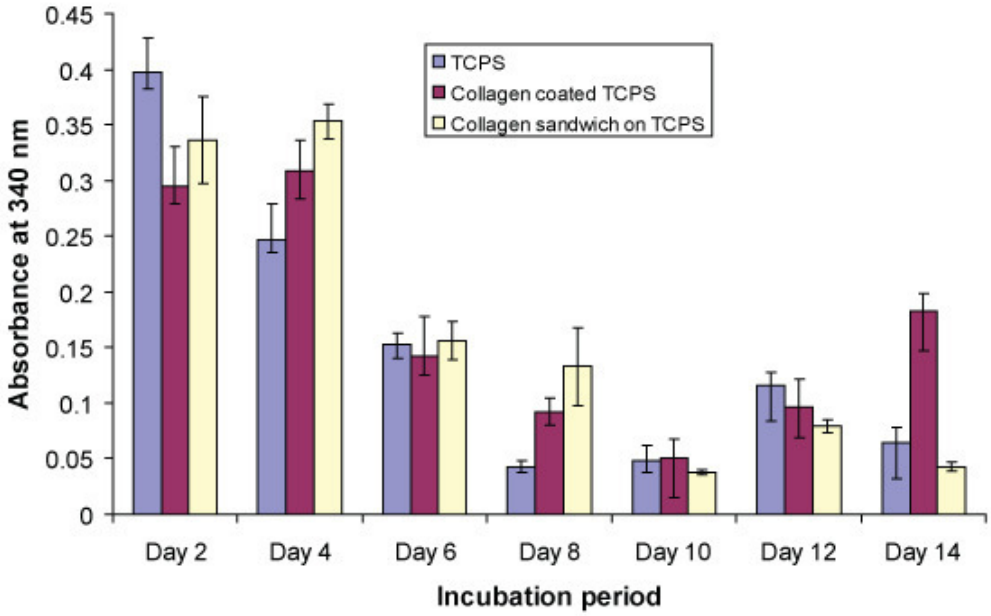

Figure 2.18 – The LDH analysis of hepatocytes attaching on modified TCPS surfaces over the 14 day incubation period. The level of LDH was determined from the media supernatant collected every 2 days via spectrophotometer measurements at 340 nm. All samples were performed in duplicates.

Previous work on the long term culture of primary hepatocytes on polyurethane/polyester matrix and polystyrene surfaces had also shown loss of viability after 3-5 days in culture without supplementation of growth factors such as epidermal growth factor (EGF)[36, 55-57]. This is consistent with our observations on our collagen deposited surfaces as urea and LDH results indicated that extensive cell apoptosis had occurred by day 6. Our maximum urea produced at day 4 from our collagen surfaces records at 20 µg/ml (see figure 2.14, day 2 and 4). This value is relatively close to some reported values in literature of between 12-18 µg per day on collagen based surface[55] while other group that use a similar seeding density reported the urea production at 44-66 µg/ml per day for each of the first 5 days[38]. A similar study was conducted by Bhatia et.al. on oxidised pSi film and had reported viability for over 2 weeks[5]. While our studies had only shown viability for only up to 5 days, it is important to highlight the fact that our starting cell density was much lower (and growth factor (EGF)

were also excluded in the study. Furthermore, the pore sizes on our surfaces were higher than those reported in Bhatia's account (2-5 nm).

2.2.3 Conclusions

To evaluate the suitability of pSi as a biomaterial, we have conducted a long term culture study of hepatocyte growing on pSi surfaces on 4 different pore sizes. Different surface modifications were also performed on the different pore sizes to investigate how both physical and chemical cues may collectively influence hepatocyte growth.

Actin fiber staining had revealed that by day 14, cells cultured on the oxidised and the APTMS surfaces had already undergone apotosis judging from the extent of cytoskeleton disorganisation. This cytoskeleton disorganisation, however, was not observed on cells cultured on collagen coated and collagen sandwich surfaces. One important finding arising from this study is the appearance of hepatocyte stacking on surfaces deposition with collagen and this was observed forming only occur on 23-38 nm surface. This stacking has also been shown convincingly for the 38 nm pSi surface by performing a Z stacking on the confocal. Stacking did not occur for smaller pore size samples or surfaces not presenting collagen. The combination of mesoporous silicon and collagen coating appears to be conducive to such cell stacking. It is well established in literature that on favorable surfaces for cellular adhesion, hepatocyte aggregation and stacking can occur[58, 59]. This behaviour is often regarded as a precursor towards the formation of hepatic cords[49] and our study may be highly useful in producing bioartificial liver constructs.

There are also several conclusions that can be drawn from the urea and LDH results. Firstly, we have demonstrated that while collagen deposition can enhance cellular longevity, both oxidised and APTMS silanised surfaces were found to be unfavorable in long term culture. Furthermore, we have also identified day 6 as the onset for the extensive cell apoptosis (by the presence of cytoskeleton disorganisation) on our pSi surface regardless of surface

modification. Finally we noticed that hepatocyte growing on surfaces with pore sizes of 23-38 nm with Rat tail type I collagen deposition were more metabolically active than cells growing on surfaces with pore sizes of 7-14 nm (see figure 2.14, day 2 and day 4). This improvement in metabolism could be related to the hepatocyte stacking as identified earlier on these pore regime.

In brief, by performing a long term culture on different porous silicon films with different pore sizes and using different approaches to present different surface chemistry and the cell adhesion mediator collagen, we have shown that chemical, biological and physical cues can collectively influence the outcome of cell culture.

References

1. Bayliss, S. C.; Buckberry, L. D.; Fletcher, I.; Tobin, M. J., The culture of neurons on silicon. ***Sensors and Actuators a-Physical*** **1999, 74, (1-3), 139-142.**

2. Bayliss, S. C.; Buckberry, L. D.; Harris, P. J.; Tobin, M., Nature of the silicon-animal cell interface. ***Journal of Porous Materials*** **2000, 7, (1-3), 191-195.**

3. Bayliss, S. C.; Heald, R.; Fletcher, D. I.; Buckberry, L. D., The culture of mammalian cells on nanostructured silicon. ***Advanced Materials*** **1999, 11, (4), 318-321.**

4. Bayliss, S. C.; Hutt, D. A.; Zhang, Q.; Harris, P.; Phillips, N. J.; Smith, A., Structural study of Porous Silicon. ***Thin Solid Films*** **1995, 255, (1-2), 128-131.**

5. Chin, V.; Collins, B. E.; Sailor, M. J.; Bhatia, S. N., Compatibility of primary hepatocytes with oxidized nanoporous silicon. ***Advanced Materials*** **2001, 13, (24), 1877-+.**

6. de-Leon, S. B. T.; Oren, R.; Spira, M. E.; Korbakov, N.; Yitzchaik, S.; Sa'ar, A., Porous silicon substrates for neurons culturing and bio-photonic sensing. ***Physica Status Solidi a-Applications and Materials Science*** **2005, 202, (8), 1456-1461.**

7. Khung, Y. L.; Barritt, G.; Voelcker, N. H., Using continuous porous silicon gradients to study the influence of surface topography on the behaviour of neuroblastoma cells. ***Experimental Cell Research*** **2008, 314, (4), 789-800.**

8. Khung, Y. L.; Graney, S. D.; Voelcker, N. H., Micropatterning of porous silicon films by direct laser writing. ***Biotechnology Progress*** **2006, 22, (5), 1388-1393.**

9. Low, S. P.; Williams, K. A.; Canham, L. T.; Voelcker, N. H., Evaluation of mammalian cell adhesion on surface-modified porous silicon. *Biomaterials* 2006, 27, (26), 4538-4546.

10. Mayne, A. H.; Bayliss, S. C.; Barr, P.; Tobin, M.; Buckberry, L. D., Biologically interfaced porous silicon devices. *Physica Status Solidi a-Applied Research* 2000, 182, (1), 505-513.

11. Pramatarova, L.; Pecheva, E.; Dimova-Malinovska, D.; Pramatarova, R.; Bismayer, U.; Petrov, T.; Minkovski, N., Porous silicon as a substrate for hydroxyapatite growth. *Vacuum* 2004, 76, (2-3), 135-138.

12. Sun, W.; Puzas, J. E.; Sheu, T. J.; Fauchet, P. M., Porous silicon as a cell interface for bone tissue engineering. *Physica Status Solidi a-Applications and Materials Science* 2007, 204, (5), 1429-1433.

13. Coffer, J. L.; Whitehead, M. A.; Nagesha, D. K.; Mukherjee, P.; Akkaraju, G.; Totolici, M.; Saffie, R. S.; Canham, L. T. In *Porous silicon-based scaffolds for tissue engineering and other biomedical applications*, 4th International Conference on Porous Semiconductors - Science and Technology (PSST-2004), Cullera, SPAIN, Mar 14-19, 2004; Cullera, SPAIN, 2004; pp 1451-1455.

14. Whitehead, M. A.; Fan, D.; Mukherjee, P.; Akkaraju, G. R.; Canham, L. T.; Coffer, J. L., High-porosity poly(epsilon-caprolactone)/mesoporous silicon scaffolds: Calcium phosphate deposition and biological response to bone precursor cells. *Tissue Engineering Part A* 2008, 14, (1), 195-206.

15. Sun, W.; Puzas, J. E.; Sheu, T. J.; Liu, X.; Fauchet, P. M., Nano- to microscale porous silicon as a cell interface for bone-tissue engineering. *Advanced Materials* 2007, 19, (7), 921-+.

16. Tsuchiya, A.; Heike, T.; Baba, S.; Fujino, H.; Umeda, K.; Matsuda, Y.; Nomoto, M.; Ichida, T.; Aoyagi, Y.; Nakahata, T., Long-term culture of postnatal mouse hepatic stem/progenitor cells and their relative developmental hierarchy. *Stem Cells* 2007, 25, (4), 895-902.

17. Yamamoto, N.; Wu, J.; Zhang, Y. H.; Catana, A. M.; Cai, H. B.; Strom, S.; Novikoff, P. M.; Zern, M. A., An optimal culture condition maintains human hepatocyte phenotype after long-term culture. *Hepatology Research* 2006, 35, (3), 169-177.

18. Ehashi, T.; Ohshima, N.; Miyoshi, H., Three-dimensional culture of porcine fetal liver cells for a bioartificial liver. *Journal of Biomedical Materials Research Part A* 2006, 77A, (1), 90-96.

19. Cyster, L. A.; Parker, K. G.; Parker, T. L.; Grant, D. M., The effect of surface chemistry and nanotopography of titanium nitride (TiN) films on 3T3-L1 fibroblasts. *Journal of Biomedical Materials Research, Part A* 2003, 67A, (1), 138-147.

20. Kapur, R.; Rudolph, A. S., Cellular and cytoskeleton morphology and strength of adhesion of cells on self-assembled monolayers of organosilanes. *Experimental Cell Research* 1998, 244, (1), 275-285.

21. Suh, J.-Y.; Jang, B.-C.; Zhu, X.; Ong, J. L.; Kim, K., Effect of hydrothermally treated anodic oxide films on osteoblast attachment and proliferation. *Biomaterials* 2002, 24, (2), 347-355.

22. Teixeira, A. I.; Abrams, G. A.; Bertics, P. J.; Murphy, C. J.; Nealey, P. F., Epithelial contact guidance on well-defined micro- and nanostructured substrates. *Journal Of Cell Science* 2003, 116, (10), 1881-1892.

23. Teixeira, A. I.; Nealey, P. F.; Murphy, C. J., Responses of human keratocytes to micro- and nanostructured substrates. *Journal of Biomedical Materials Research, Part A* 2004, 71A, (3), 369-376.

24. Khung, Y. L.; McInnes, S.; Cole, M. A.; Voelcker, N. H., Control over wettability via surface modification of porous gradients. *Proceedings of SPIE-The International Society for Optical Engineering* 2007, 6799.

25. Stewart, M. P.; Buriak, J. M., Chemical and biological applications of porous silicon technology. *Advanced Materials* 2000, 12, (12), 859-869.

26. Sangsanoh, P.; Waleetorncheepsawat, S.; Suwantong, O.; Wutticharoenmongkol, P.; Weeranantanapan, O.; Chuenjitbuntaworn, B.; Cheepsunthorn, P.; Pavasant, P.; Supaphol, P., In vitro biocompatibility of schwann cells on surfaces of biocompatible polymeric electrospun fibrous and solution-cast film scaffolds. *Biomacromolecules* 2007, 8, (5), 1587-1594.

27. Khademhosseini, A.; Suh, K. Y.; Yang, J. M.; Eng, G.; Yeh, J.; Levenberg, S.; Langer, R., Layer-by-layer deposition of hyaluronic acid and poly-L-lysine for patterned cell co-cultures. *Biomaterials* 2004, 25, (17), 3583-3592.

28. Gao, T.; Gao, J.; Sailor, M. J., Tuning the response and stability of thin film mesoporous silicon vapor sensors by surface modification. *Langmuir* 2002, 18, (25), 9953-9957.

29. Janshoff, A.; Dancil, K.-P. S.; Steinem, C.; Greiner, D. P.; Lin, V. S. Y.; Gurtner, C.; Motesharei, K.; Sailor, M. J.; Ghadiri, M. R., Macroporous p-Type Silicon Fabry-Perot Layers. Fabrication, Characterization, and Applications in Biosensing. *Journal of the American Chemical Society* 1998, 120, (46), 12108-12116.

30. Xu, D.; Sun, L.; Li, H.; Zhang, L.; Guo, G.; Zhao, X.; Gui, L., Hydrolysis and silanization of the hydrosilicon surface of freshly prepared porous silicon by an amine catalytic reaction. *New Journal of Chemistry* 2003, 27, (2), 300-306.

31. Suzuki, A.; Tsutomi, Y., Inductions of fibroblast-like morphology and high growth activity by low-dose CPT-11 in PC12 cells: role of tenascin. *Toxicology in Vitro* 2000, 14, (4), 337-343.

32. Song, J.; Chen, J.; Klapperich, C. M.; Eng, V.; Bertozzi, C. R., Functional glass slides for in vitro evaluation of interactions between osteosarcoma TE85 cells and mineral-binding ligands. *Journal of Materials Chemistry* 2004, 14, (17), 2643-2648.

33. Hung, C. H.; Young, T. H., Differences in the effect on neural stem cells of fetal bovine serum in substrate-coated and soluble form. *Biomaterials* 2006, 27, (35), 5901-5908.

34. Valentiner, U.; Carlsson, M.; Erttmann, R.; Hildebrandt, H.; Schumacher, U., Ligands for the peroxisome proliferator-activated receptor-gamma have inhibitory effects on growth of human neuroblastoma cells in vitro. *Toxicology* 2005, 213, (1-2), 157-168.

35. Fiegel, H. C.; Kaufmann, P. M.; Bruns, H.; Kluth, D.; Horch, R. E.; Vacanti, J. P.; Kneser, U., Hepatic tissue engineering: from transplantation to customized cell-based liver directed therapies from the laboratory. *Journal of Cellular and Molecular Medicine* 2008, 12, (1), 56-66.

36. Poyck, P. P. C.; Hoekstra, R.; van Wijk, A.; Attanasio, C.; Calise, F.; Chamuleau, R.; van Gulik, T. M., Functional and morphological comparison of three primary liver cell types cultured in the AMC bioartificial liver. *Liver Transplantation* 2007, 13, (4), 589-598.

37. Barbich, M.; Lorenti, A.; Hidalgo, A.; Ielpi, M.; de Santibanez, M.; de Santibanez, E.; Morales, V.; Marin, M. C.; Callero, M. F.; Argibay, P. F., Culture and characterization of human hepatocytes obtained after graft reduction for liver transplantation: A reliable source of cells for a bioartificial liver. *Artificial Organs* 2004, 28, (7), 676-682.

38. De Bartolo, L.; Salerno, S.; Morelli, S.; Giorno, L.; Rende, M.; Memoli, B.; Procino, A.; Andreucci, V. E.; Bader, A.; Drioli, E., Long-term maintenance of human hepatocytes in oxygen-permeable membrane bioreactor. *Biomaterials* 2006, 27, (27), 4794-4803.

39. Pasquale, V.; Massobrio, P.; Bologna, L. L.; Chiappalonea, M.; Martinoia, S., Self-organization and neuronal avalanches in networks of dissociated cortical neurons. *Neuroscience* 2008, 153, (4), 1354-1369.

40. Liu, B. F.; Ma, J.; Gao, E. J.; He, Y.; Cui, F. H.; Xu, Q. Y., Development of an artificial neuronal network with post-mitotic rat fetal hippocampal cells by polyethylenimine. *Biosensors & Bioelectronics* 2008, 23, (8), 1221-1228.

41. Du, Y.; Han, R. B.; Wen, F.; San, S. N. S.; Xia, L.; Wohland, T.; Leo, H. L.; Yu, H., Synthetic sandwich culture of 3D hepatocyte monolayer. *Biomaterials* 2008, 29, (3), 290-301.

42. Nahmias, Y.; Kramvis, Y.; Barbe, L.; Casali, M.; Berthiaume, F.; Yarmush, M. L., A novel formulation of oxygen-carrying matrix enhances liver-specific function of cultured hepatocytes. *Faseb Journal* 2006, 20, (14), 2531-+.

43. Clements, L. R.; Khung, Y. L.; Thissen, H.; H, V. N., 2-directional gradient substrates for subsequent studies of cell-surface interaction. *Proceedings of SPIE-The International Society for Optical Engineering* 2007, 6799.

44. Salonen, J.; Bjorkqvist, M.; Laine, E.; Niinisto, L., Effects of fabrication parameters on porous p(+)-type silicon morphology. *Physica Status Solidi a-Applied Research* 2000, 182, (1), 249-254.

45. Harada, H.; Shirahashi, T.; Nakamura, M.; Ohwada, T.; Sasaki, Y.; Okuda, S.; Hosono, A., Macropore formation in anodized p-type silicon. *Japanese Journal of Applied Physics Part 1-Regular Papers Short Notes & Review Papers* 2001, 40, (8), 4862-4863.

46. Janshoff, A.; Dancil, K. P. S.; Steinem, C.; Greiner, D. P.; Lin, V. S. Y.; Gurtner, C.; Motesharei, K.; Sailor, M. J.; Ghadiri, M. R., Macroporous p-type silicon Fabry-Perot layers. Fabrication, characterization, and applications in biosensing. *Journal of the American Chemical Society* 1998, 120, (46), 12108-12116.

47. Novikoff, P. M.; Cammer, M.; Tao, L.; Oda, H.; Stockert, R. J.; Wolkoff, A. W.; Satir, P., Three-dimensional organization of rat hepatocyte cytoskeleton: Relation to the asialoglycoprotein endocytosis pathway. *Journal of Cell Science* 1996, 109, 21-32.

48. Nishikawa, Y.; Tokusashi, Y.; Kadohama, T.; Nishimori, H.; Ogawa, K., Hepatocytic cells form bile duct-like structures within a three-dimensional collagen gel matrix. *Experimental Cell Research* 1996, 223, (2), 357-371.

49. Sudo, R.; Mitaka, T.; Ikeda, M.; Tanishita, K., Reconstruction of 3D stacked-up structures by rat small hepatocytes on microporous membranes. *FASEB Journal* 2005, 19, (10), 1695-+.

50. Lin, C. C.; Hung, K. C.; Young, T. H.; Chen, Y. S.; Yong, C. C.; Kobayashi, E.; Wu, C. H.; Yang, C. H.; Chen, C. L.; Wang, C. C., Influence of hypothermic conditions on primary porcine hepatocyte-entrapped hollow fiber bioreactors. *Biochemical Engineering Journal* 2006, 29, (1-2), 139-148.

51. Lagadic-Gossmann, D.; Rissel, M.; Le Bot, M. A.; Guillouzo, A., Toxic effects of tacrine on primary hepatocytes and liver epithelial cells in culture. *Cell Biology and Toxicology* 1998, 14, (5), 361-373.

52. Esteve, M. A.; Carre, M.; Braguer, D., Microtubules in apoptosis induction: Are they necessary? *Current Cancer Drug Targets* 2007, 7, (8), 713-729.

53. Cabado, A. G.; Leira, F.; Vieytes, M. R.; Vieites, J. M.; Botana, L. M., Cytoskeletal disruption is the key factor that triggers apoptosis in okadaic acid-treated neuroblastoma cells. *Archives of Toxicology* 2004, 78, (2), 74-85.

54. Glicklis, R.; Shapiro, L.; Agbaria, R.; Merchuk, J. C.; Cohen, S., Hepatocyte behavior within three-dimensional porous alginate scaffolds. *Biotechnology and Bioengineering* 2000, 67, (3), 344-353.

55. Higuchi, A.; Satoh, M.; Kobayashi, K.; Cho, C. S.; Akaike, T.; Tak, T. M.; Egashira, S.; Matsuoka, Y.; Natori, S. H., Albumin and urea production by hepatocytes cultured on polyurethane foaming membranes coated with extracellular matrix. *Journal of Membrane Science* 2006, 280, (1-2), 983-989.

56. Washizu, J.; Berthiaume, F.; Chan, C.; Tompkins, R. G.; Toner, M.; Yarmush, M. L., Optimization of rat hepatocyte culture in citrated human plasma. *Journal of Surgical Research* 2000, 93, (2), 237-246.

57. Donato, M. T.; Ponsoda, X.; O'Connor, E.; Castell, J. V.; Gomez-Lechon, M. J., Role of endogenous nitric oxide in liver-specific functions and survival of cultured rat hepatocytes. *Xenobiotica* 2001, 31, (5), 249-264.

58. Abu-Absi, S. F.; Friend, J. R.; Hansen, L. K.; Hu, W. S., Structural polarity and functional bile canaliculi in rat hepatocyte spheroids. *Experimental Cell Research* 2002, 274, (1), 56-67.

59. Abu-Absi, S. F.; Hu, W. S.; Hansen, L. K., Dexamethasone effects on rat hepatocyte spheroid formation and function. *Tissue Engineering* 2005, 11, (3-4), 415-426.